SEMMELWEIS EGYETEM
DOKTORI ISKOLA

Ph.D. értekezések

3415.

MIKOLICZ ÁKOS

Fogorvostudományi kutatások
című program

Programvezető: Dr. Varga Gábor, egyetemi tanár
Témavezető: Dr. Vág János, egyetemi tanár

Reliability of digital impressions for human identification based on palatal structures

PhD thesis

Ákos Mikolicz DMD

Division of Dental Research
Semmelweis University Doctoral College

Supervisor: János Vág, DMD, DSc
Official reviewers: Bálint Vecsei, DMD, PhD
Balázs Sándor, DMD, PhD

Head of the Complex Examination Committee:

István Gera, DMD, PhD

Members of the Complex Examination Committee:

Gábor Gerber, DMD, PhD,

Ákos Károly Nagy, DMD, PhD

Budapest
2026

TABLE OF CONTENTS

LIST OF ABBREVIATIONS 5

1 INTRODUCTION 6

1.1 Palatal rugae 7

1.2 Palatal rugae as a basis for human identification 8

1.3 Intraoral scanners and human identification 9

1.4 Palatal geometry 10

1.5 Further aspects of the palate-based identification 11

1.6 Methods for evaluating the palatal-based discriminative potential of intraoral scans 12

2 OBJECTIVES 13

3 METHODS 15

3.1 Study 1: *„Reproducibility of the digital palate in forensic investigations: a two-year retrospective cohort study on twins”* 15

3.1.1 Subject selection 15

3.1.2 Palatal scanning 15

3.1.3 Data analysis 16

3.1.4 Statistics 18

3.2 Study 2: *„Human identification via digital palatal scans: a machine learning validation pilot study”* 18

3.2.1 Measurement of the palatal vault geometry 20

3.2.2 Identification based on geometry 22

3.2.3 Identification based on scan superimposition 22

3.2.4 Sex determination based on geometry 23

3.2.5 Statistical analysis 24

4 RESULTS 25

4.1 Study 1: *„Reproducibility of the digital palate in forensic investigations: a two-year retrospective cohort study on twins”* 25

4.1.1 The effect of orthodontic treatment and the comparison area on forensic reproducibility 25

4.1.2 The effect of the digitization method on forensic and technical reproducibility 27

4.1.3 Stability of the anterior palatal area over a two-year period 29

4.1.4 The discriminative potential of anterior palatal scans using an IOS 30

4.2 Study 2: *„Human identification via digital palatal scans: a machine learning validation pilot study”* 32

4.2.1 Identification based on palatal geometry 32

4.2.2 Identification based on scan superimposition 33

4.2.3 Sex determination based on geometry 35

5 DISCUSSION 36

5.1 Different digitization methods and reproducibility 38

5.2 The potential impact of orthodontic treatment 41

5.3 Identification based on palatal geometry and by superimposition of digital scans 42

5.4 Sex determination based on palatal geometry and superimposition of digital scans 44

5.5 An implication for ethnic differentiation based on palatal geometry 45

5.6 Strengths and limitations 45

5.7 Future advancements and considerations 48

6 CONCLUSIONS 50

7 SUMMARY 51

8 REFERENCES 52

9 BIBLIOGRAPHY OF PUBLICATIONS 65

9.1 Publications related to the thesis: 65
9.2 Publications not related to the thesis 66
10 ACKNOWLEDGEMENTS 67

LIST OF ABBREVIATIONS

BHP – Bottom horizontal plane
CI – Confidence interval
CP – Central point
DNA – Deoxyribonucleic acid
DVI – Disaster victim identification
ESA – Emerald S „A" software version
ESB – Emerald S „B" software version
GYPS – Dental stone cast (gypsum model)
IOS – Intraoral scanner
IP – Incisive papilla
LAB – Laboratory scanner
LM – Left molar
LDA – Linear discriminant analysis
MAD – Mean absolute distance
MZ – Monozygotic
PS – Primescan intraoral scanner
RM – Right molar
SD – Standard deviation
SEM – Standard error of mean
STL – Standard triangulation language
THP – Top horizontal plane
2D – Two-dimensional
3D – Three-dimensional

1 INTRODUCTION

In the event of a natural disaster, forensic experts encounter significant challenges in identifying the victims (1). For example, following the 2004 Asian earthquake and tsunami, identifying more than 200,000 victims proved to be an extremely demanding task. This project required careful effort and resources, highlighting the significant scale and complexity of the operation (2-5). A more recent mass disaster in Turkey in 2023 resulted in the death of more than 56,000 people, which also posed significant challenges in terms of identifying the victims (6).

It is important to acknowledge the potential for an increase in natural disasters worldwide, including floods, earthquakes, and tsunamis, as a result of extreme weather conditions caused by climate change (7).

According to the Interpol standard for Disaster Victim Identification (DVI), methods employed for human identification in disaster situations must be scientifically validated, dependable, practical for field conditions, and feasible to execute within a reasonable timeframe (8). The primary and most dependable techniques are friction ridge (fingerprint) analysis, deoxyribonucleic acid (DNA) testing and comparative dental analysis (8).

Recording fingerprints can present certain challenges in the context of disaster victim identification. In many cases, fingerprints may be damaged, which can limit their use for forensic purposes (9, 10). Often, fingers are the first body parts to be harmed in an accident, which prevents them from being used for identification (11).

Analyzing DNA can be costly (9), time-consuming (12) and cross-contamination of DNA fragments is possible during examination, which may mislead forensic experts (13). In forensic science, dental records are one of the most used methods for identifying individuals after death (3, 14-16). Nevertheless, identifying individuals through their dental records has its limitations since teeth undergo continual changes throughout a person's lifetime (17, 18).

1.1 Palatal rugae

The palatal rugae, which are the ridges on the roof of the mouth, are thought to create a unique pattern, much like a fingerprint (19). Palatal rugae initiate their development during the third month of intrauterine life, originating from connective tissue that covers the palatine process of the maxillary bone (20). The formation and growth of these structures are subject to regulation by interactions between epithelial and mesenchymal cells. These cells express specific molecules within the extracellular matrix during the developmental process (21-23).

The functions of the palatal rugae include aiding in the movement of food through the oral cavity, preventing food loss from the mouth, and assisting with the chewing process. Thanks to the presence of gustatory and tactile receptors, they also play a role in perceiving taste, assessing the texture of food, and determining tongue position (1, 24, 25).

According to reports, the number of rugae remains unchanged during early preadolescence and adolescence (26, 27). Throughout an individual's life, they may undergo changes in size; however, their shape remains relatively constant (21, 28-30). Because the hard palate is protected by the alveolar arch, teeth, cheeks, and lips, the risk of damage from trauma is significantly lower than that for DNA or fingerprints (31). Furthermore, the rugae are capable of enduring heat and chemicals thanks to the effective protection provided by the skull (27, 32, 33). Even in the case of a burnt body, the palatal rugae remain relatively intact (34).

It is worth mentioning that palatal rugae are often used as reference points in measuring tooth migration in orthodontic therapy (35, 36), although this method is not universally accepted (28). In addition, they might have an influence on therapy planning in prosthodontic dentistry (36). They can also aid in diagnosing and identifying submucosal clefts in the palate, as specific morphometric patterns of palatal rugae may indicate the existence of such clefts (36, 37).

Several morphological differences have been reported between the two sexes. In men, palatal rugae more often extend into the posterior third and show more distinctive features than in women (38). Women have more consistent but fewer discriminatory coordinates compared to men (39). In humans, palatal rugae are asymmetrical, which is unique to human beings (1, 40). The number and distribution of primary rugae do not exhibit

bilateral symmetry from the midline. Studies have shown that males tend to have a slightly higher number of rugae, and in both sexes, there is a tendency for more rugae to be present on the left side (1, 28).

There are, however, several factors that may influence the morphology of the rugae. Regarding the effect of orthodontic treatment, the literature is rather controversial (41-44). Peavy and Kendrick observed that the rugae located closer to the teeth are more inclined to stretch in the same direction as the movement of the associated teeth (1, 45). The question arises whether changes to the rugae after orthodontic treatment are significant enough to prevent their use for human identification.

Extractions may also affect the direction of rugae near the extraction site (46). Nevertheless, it has been shown in several studies that in extraction cases, the rugae in general are stable and it has also been observed that medial points are more stable than lateral points (35, 47, 48).

1.2 Palatal rugae as a basis for human identification

In 1888, Allen was the first to suggest using the palatal rugae patterns for identification (49). Since then, several investigations have indicated that palatal rugae imprints may have a significant role in human identification (1, 19, 21, 32, 38, 50-55). Although this hypothesis has not been universally accepted, numerous studies suggest that rugae patterns show uniqueness between individuals (1, 21, 38, 56, 57).

It is important to note that in situations where the victim is completely edentulous, the only dental feature for identification may be the palatal rugae (52, 58).

In the scientific literature, studying the palatal rugae for identification is often referred to as rugoscopy or palatoscopy (59-63).

An important finding is that palatal rugae remain resistant to decomposition changes for up to seven days postmortem (after death) under optimal storage conditions (34).

Acquiring antemortem (before death) data in a forensic investigation can be particularly difficult, especially when it comes to identifying disaster victims. Unlike fingerprints and DNA, there is a higher likelihood of finding a dental record that includes the rugae pattern. Reference data can be dental casts, intraoral photographs (64), removable dentures (32, 58), or even intraoral scans (65, 66).

It is interesting to note that there have been previous attempts to use the palatal rugae for paternity testing. However, this did not prove to be a reliable method (67).

1.3 Intraoral scanners and human identification

Intraoral scanners (IOSs) can be extensively used to capture the shape of teeth and the palatal rugae in digital form (18, 68). Taneva et al. (69) were pioneers in employing a three-dimensional (3D) assessment technique to analyze rugae patterns for individual differentiation. They examined the differences between two-dimensional (2D) measurements (taken from sections) and the 3D variations of the medial and lateral endpoints of the rugae using digitized alginate impressions, plaster models, and direct intraoral scans. Their findings indicate that the 3D method is more dependable for human identification compared to the 2D approach. In a case study (70), a pair of twins was effectively differentiated by utilizing the 3D rugae landmark method along with an iTero intraoral scanner (Align Technology, Inc., San Jose, CA, USA).

IOSs have become a rapid and portable option for data collection during large-scale disasters, though their application in investigative settings is still limited.

A previous cohort study that was conducted by our research team with 104 twins (65) established that a palatal intraoral scan serves as an effective tool for distinguishing individuals through whole-surface comparisons or geometric measurements. We proposed that if identical twins, who share the same genotype and phenotype, can be objectively differentiated, this method could potentially be utilized on a larger scale—possibly even across the general population—to distinguish between all humans, including relatives and strangers (11, 65). From a statistical perspective, we hypothesized that the reproducibility of the IOS should exceed the differences observed between monozygotic (MZ) twin siblings. This hypothesis was confirmed by successfully replicating the palate using the same IOS (65). However, the accuracy of palatal scanning—both trueness and precision—might differ between direct digitization using either the same or different IOSs and indirect digitization from conventional impressions (via a laboratory scanner) (69, 71-73).

1.4 Palatal geometry

The anatomical geometry of the human palate is influenced by genetic, environmental, and developmental factors (74, 75), showing considerable differences among various populations (76-78).

In a study (11) carried out by our research team, we made a significant discovery showcasing the effectiveness of using an IOS for accurately identifying individuals based on palatal geometry. A supervised machine learning algorithm was effectively created and evaluated using height, width, and depth as variables, specifically in a Caucasian population from Hungary. However, training the machine learning model on a homogeneous population may lead to overfitting, lowering its accuracy on other populations (e.g., the test set). Therefore, a critical question remains: Can this algorithm produce equally reliable results when applied to a larger, more diverse test population? The consequences for forensic practice can only be realized if it demonstrates applicability without any restrictions.

The superimposition of intraoral scans is extremely precise and reliable, and is commonly used in digital dentistry to assess accuracy (79, 80). Research has indicated (56, 65, 69, 81, 82) that palatal-scan superimposition can be used for identification. IOSs show great potential for advancing forensic dentistry and 3D comparisons in the future (83-85).

The alignment algorithm, however, is time-consuming and not suitable for searching through a large database. It has recently been suggested that the alignment of two palatal scans is mainly influenced by the geometry of the palatal vault instead of the surface features, such as the palatal rugae (11). Geometric data, which encompasses the height, width, and depth of the palatal vault, occupies less storage space and enables faster searches and matching within databases. As a result, using geometric-based identification may serve as a viable alternative to the superimposition method, particularly in cases where the rugae pattern degrades postmortem. To validate this concept, a linear discriminant function was created by our research team using height, width, and depth as parameters to differentiate individuals and ascertain sex (11). The coefficients for the three variables were established within a Caucasian population from the same country (i.e. Hungary). The discriminant function demonstrated a high success rate in identifying an individual's scan, achieving 91.2% sensitivity and 97.8% specificity. However, using

the same training set for a new classification function can lead to biased results and an overestimation of accuracy (i.e., it may be overfitting) when relying on internal validation (86). Consequently, it is crucial to conduct external validation of a machine learning model prior to its application in real-world situations (87, 88).

1.5 Further aspects of the palate-based identification

In a forensic investigation, particularly in the context of disaster victim identification, the victims may originate from various countries, representing different populations (3, 5). Furthermore, research has shown that there are variations in the anatomy of the rugae among individuals from different countries (26, 76-78, 89-94). As a result, the previously established discriminant function designed for a homogeneous population may not perform well in a mixed population due to differences in dimensional characteristics between the training and test sets.

There has been some confusion in the scientific field regarding the correct use of terms such as *ethnicity*, *race*, and *ancestry*. Often, these expressions are used synonymously; however, they should be used appropriately (95, 96).

Ethnicity is a multi-factorial concept rooted in shared cultural characteristics such as language, nationality, history, and religion. In general, ethnicity should be determined by self-identification (95, 97, 98).

Race should be considered as a social construct based on physical characteristics like skin tone and hair texture (95, 99).

Ancestry refers to the biological roots of a person, encompassing genetic, genealogical, and geographical factors (95, 100).

Determining the sex of an individual is essential for identifying victims (101, 102). In the above-mentioned machine learning-based study, it was found that using palatal geometry for sex determination yielded moderate accuracy, with a sensitivity of 82.2% and specificity of 89,3% (11). The effectiveness of this method may decrease even more in mixed populations because of variations in palatal size across different groups.

1.6 Methods for evaluating the palatal-based discriminative potential of intraoral scans.

Different methods for comparing intraoral palatal scans for forensic purposes have been previously described:

1. *The superimposition-based method* calculates the deviation values between two scans by overlaying them using the iterative closest point algorithm (18, 27, 65, 103).
2. *The palatal rugae pattern recognition method* uses an automated algorithm or manual selection to extract the palatal ridges for further comparison (19, 104).
3. *Geometry-based method*: In this case, the different dimensions of the palatal vault (height, depth, and width) are compared and used to match the scans (11, 103, 105).

Some important phrases in this thesis require explanation. *Repeatability* refers to the comparison of scans made by the same scanner in the same session (27). We introduced two terms that were previously not present in the forensic science literature in order to describe different types of reproducibility: 'technical reproducibility' and 'forensic reproducibility' (27).

Technical reproducibility refers to the comparison of scans taken by different scanners during the same session.

Forensic reproducibility, on the other hand, refers to the comparison of scans taken at different times using different scanners. This simulates a real-life scenario in which ante-mortem and postmortem scans are taken at different times using different devices.

2 OBJECTIVES

The morphology of the human palate, particularly the anterior region (palatal rugae), differs from person to person and may be useful for identifying individuals using digital methods, such as intraoral scanners. However, relatively little scientific data exists on this identification method. Many questions need to be addressed: Can different types of intraoral scanners be used for this purpose? Does orthodontic treatment significantly affect palatal morphology? Does time influence the results? To answer these questions, we conducted two studies.

Study 1: Reproducibility of the digital palate in forensic investigations: a two-year retrospective cohort study on twins

The aims of this study were:

1. to assess the effects of orthodontic treatment on forensic reproducibility
   Null hypothesis #1: Orthodontic treatment has no effect on forensic reproducibility.
2. to assess the effect of comparison area selection (complete or anterior palate) on forensic reproducibility
   Null hypothesis #2: The selection of the comparison area has no effect on forensic reproducibility.
3. to investigate the effect of the digitization method on forensic reproducibility (different scanners at different times)
   Null hypothesis #3: The digitization method has no effect on forensic reproducibility.
4. to investigate the effect of the digitization method on technical reproducibility (different scanners at the same time)
   Null hypothesis #4: The digitization method has no effect on technical reproducibility.
5. to evaluate palatal stability by comparing differences between monozygotic twin siblings measured at the baseline and two years later.

Null hypothesis #5: There is no change in the differences between MZ twins over two years.

6. to assess the discriminative potential of the palatal scans by comparing the forensic reproducibility of the individual subjects to the between-sibling difference

   Null hypothesis #6: The forensic reproducibility and the between-sibling difference do not vary.

Study 2: Human identification via digital palatal scans: a machine learning validation pilot study

The aims of this study were:

7. to perform an external validation of a previously developed and published palatal geometry-based discrimination algorithm on a different population

   Null hypothesis #7: The accuracy of the palatal geometry-based discrimination algorithm does not change in the test population.

8. to perform an external validation of a previously developed and published superimposition-based discrimination algorithm on a different population

   Null hypothesis #8: The accuracy of the superimposition-based discrimination algorithm does not change in the test population.

9. to perform an external validation of a previously developed and published sex determination algorithm on a different population.

   Null hypothesis #9: The accuracy of the sex determination does not change in the test population.

3 METHODS

3.1 Study 1: *„Reproducibility of the digital palate in forensic investigations: a two-year retrospective cohort study on twins"*

3.1.1 Subject selection

A total of 20 sets of monozygotic twins (40 individuals) were initially scanned in 2019 (65) and were rescanned in 2021 using five different methods. The scans conducted in 2019 represented simulated antemortem (before death) data, while those in 2021 provided simulated postmortem (after death) data. Some papers suggest that orthodontic treatment could alter palatal morphology (41, 106). Given that younger individuals are more likely to undergo orthodontic treatment and experience physical growth, 20 young monozygotic twins (40 individuals) were selected for the 2021 session from the original group of 64 monozygotic twins scanned in 2019. The inclusion criteria specified that participants had to have three error-free intraoral scans from 2019, be aged between 18 and 32 years, and attend the session together with their sibling. Additionally, individuals with missing maxillary teeth (other than the second and third molars), those having orthodontic devices on the palate, or a history of forced maxillary expansion between sessions were excluded. All procedures adhered to the Declaration of Helsinki. Informed consent was obtained from all subjects. Ethical approval was obtained from the National Health Registration and Training Center on July 26, 2018 (approval number: 36699–2/2018/EKU).

3.1.2 Palatal scanning

In 2019, every participant underwent three scans using an Emerald IOS (software version 5.2.1, Planmeca, Helsinki, Finland), referred to as E. In 2021, the participants were scanned using Emerald S intraoral scanners (Planmeca, Helsinki, Finland) with two different software versions (6.3.2.12 and 6.3.1.6), as well as Primescan (software version 5.1.3.7, Dentsply Sirona, Charlotte, North Carolina, USA), indicated as ESA, ESB, and PS, respectively. Two indirect digitization techniques were utilized. The first involved creating a traditional vinyl polysiloxane impression (Virtual 380, Ivoclar, Schaan,

Lichtenstein) using a stock plastic impression tray. This impression was then digitized with a laboratory scanner (Planscanlab, 5.0, Planmeca, Helsinki, Finland), referred to as LAB. Following this, the impression was cast in Type IV dental plaster (Lean Rock, Whipmix, Louisville, USA). Finally, the plaster model was scanned with Planscanlab to produce gypsum scanning (GYPS) data sets.

3.1.3 Data analysis

The comparison between any two scans was conducted by superimposing them. Initially, both scans were loaded into the GOM Inspect® engineering analysis software (Suite 2020, GOM GmbH, Braunschweig, Germany), where best-fit alignment was applied using the iterative closest point algorithm. This algorithm aimed to minimize the total distance by positioning the surface points of the scans as closely as possible. The minimized distance is represented as the mean absolute distance (MAD). The design of the study was as follows: (Fig. 1):

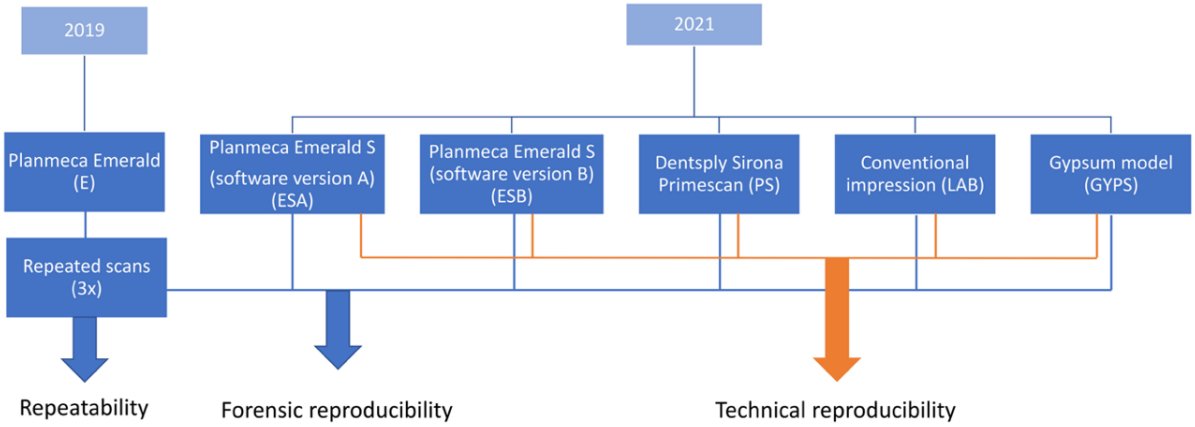

Fig. 1. Study design. Repeatability was assessed by aligning the three Emerald scans for each individual taken in 2019. Following that, forensic reproducibility was determined by aligning the 2021 scans obtained with five different scanning devices to one of the three Emerald scans from 2019. Lastly, technical reproducibility was evaluated by aligning the Emerald S (ESA) scans with the other scans conducted in 2021. (E: Emerald scanner, ESA: Emerald S scanner with software version 'A', ESB: Emerald scanner with software version 'B', PS: Primescan, GYPS: gypsum model, LAB: laboratory scanner) (27)

1. Forensic reproducibility was determined by aligning the scans taken in 2021 from three different intraoral scanners (ESA, ESB, PS) and two indirect techniques (LAB, GYPS) with one of the three Emerald scans from 2019 (E). This approach led to five combinations: E_ESA, E_ESB, E_PS, E_LAB, and E_GYPS. An antemortem/postmortem simulation involving 200 samples was conducted, incorporating all variables such as aging, orthodontic treatment, and scanner types.

2. Repeatability was assessed by aligning the three Emerald scans of each individual from 2019. (E_E, n=120).

3. Within the GOM Inspect® software, the scans were cropped to exclude the palatal gingiva, incisal papilla, and the posterior region of the palate. The cropping was limited to the most distally positioned rugae. As a result, the following analyses were conducted using only the anterior section of the palate.

4. The comparisons for forensic reproducibility (point 1) and repeatability (point 2) were redone after only the anterior section of the palate was retained.

5. Technical reproducibility was assessed by aligning the ESA scans with the scans from the other intraoral scanners used in 2021 (ESA-ESB, ESA-PS, ESA-LAB, ESA-GYPS, n=160).

6. The impact of time on the discriminatory capability of the palate scan was assessed by analyzing the differences between twin siblings measured in 2019 and 2021. This was achieved by superimposing the intraoral scans of 20 pairs of twins from 2019 (E_E) and 2021 (ESA_ESA, PS_PS), leading to a total of 60 comparisons.

3.1.4 Statistics

The sample size was determined based on findings from our previous study (65) and some estimations. In that study, the Emerald scanner demonstrated a precision of 35.3 μm with a standard deviation of 14 μm for palatal scans. However, we lacked data on the deviations between palatal scans produced by different scanners. To provide a comparative estimate for scans from various scanners, we used a precision value of 73 μm and a standard deviation of 26 μm, both measured in 2019 (65), effectively doubling the original values.

To differentiate between individuals, it was important that the lower tolerance interval of the deviation between siblings and the upper tolerance interval of reproducibility did not overlap. The previous study reported a between-siblings difference of 411±90 μm (65). With a 95% confidence level and a 95% tolerance (population coverage), we required 11 pairs of twins. For a 99% tolerance level, we would need 47 pairs, which was unfeasible due to the inclusion and exclusion criteria, as well as the need to recall all 64 monozygotic twins from 2019. Thus, we opted for 95% tolerance and invited as many pairs as possible.

The impacts of orthodontic treatment, the comparison area (complete palate vs. anterior), and the scanning technique on the mean absolute distance (MAD) were analyzed using a generalized linear mixed model with a gamma distribution and a log-link function. Additionally, the MAD values between siblings obtained from different scanners were compared using a Kruskal-Wallis nonparametric test. Significance levels for multiple comparisons were adjusted using the Bonferroni correction. All analyses were conducted using SPSS version 28 (IBM).

3.2 Study 2: *„Human identification via digital palatal scans: a machine learning validation pilot study"*

The second study we conducted was a cross-sectional observational study. It was retrospectively registered on ClinicalTrials.gov, with the registration number NCT05349942 (dated 27/04/2022). Participants were recruited from postgraduate students attending a one-week methodological research training course at Semmelweis University, who provided their scanned data anonymously. The investigators did not influence the selection of participants, their countries of origin, or the distribution of sex.

Upon arrival, no specific inclusion or exclusion criteria were applied other than obtaining consent to participate, to prevent any deliberate enhancement of the accuracy of the discrimination algorithms. The participants represented a unique cohort that simulated a real forensic scenario, such as a disaster situation. The study included twenty-three participants (16 females and 7 males) aged between 23 and 35, hailing from 11 different countries in Asia and Europe. (Table 1).

Table 1. Countries of origin with sample numbers (103)
(N: north, E: east, W: west)

	Longitude and latitude (capital city)	Female	Male	Sum
Belgium	50.85° N, 4.35° E	1	0	1
Bulgaria	42,69° N, 23,32° E	1	0	1
China	39.9° N, 116,391° E	0	2	2
Croatia	45.8° N, 15,99° E	0	2	2
Germany	52.52° N, 13.41° E	1	1	2
Greece	37.59° N, 23.43° E	2	0	2
Hungary	47.49° N, 19.04° E	1	0	1
Iran	35.68° N, 51.38° E	1	0	1
Italy	41.9° N, 12.5° E	0	1	1
Portugal	38.72° N, -9,15° W	2	0	2
Turkey	39.9° N, 32.81° E	7	1	8
Sum		16	7	23

Written informed consent was obtained from the participants, and the study was carried out according to the Declaration of Helsinki. Ethical approval was granted from the national committee (36699-2/2018/EKU). The method protocol is summarized in a flowchart (Fig. 2).

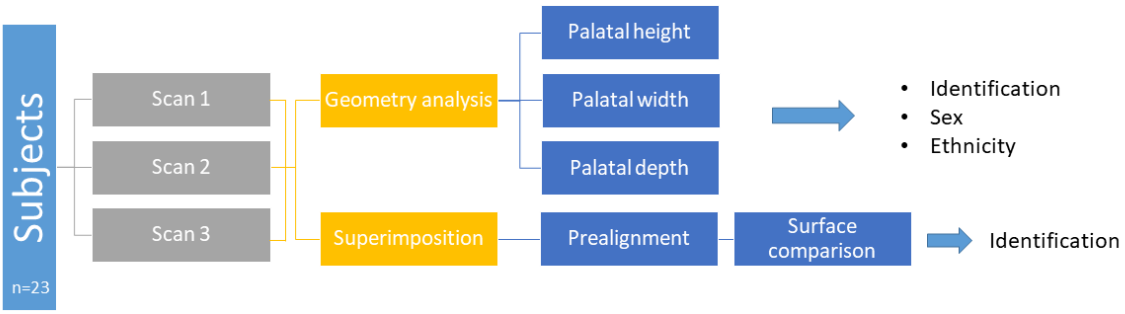

Fig. 2. The study protocol summarized in a flowchart. All 23 participants underwent three scans, after which both geometry- and superimposition-based comparisons were applied. For the geometry-based method, palatal dimensions were evaluated for identification purposes and to determine sex and ethnicity. The superimposition-based method was only used for identification. (103)

Each participant underwent three scanning sessions. A key aspect of the scanning procedure was following a specific zigzag pattern using the Planmeca Emerald IOS (software version 6.2.1.19, Planmeca, Helsinki, Finland), beginning at the incisive papilla. The geographic coordinates (longitude and latitude) of each participant's country were documented, and the differences in coordinates between the two subjects were used to evaluate population diversity.

3.2.1 Measurement of the palatal vault geometry

The height, depth, and width measurements were conducted following the guidelines set by Simon et al. (11) using GOM Inspect software (GOM GmbH, Braunschweig, Germany). Palatal width was defined as the distance between the palatal grooves of the right first molar (RM) and the left first molar (LM) at the gingival margin level (see Fig. 3A). Depth was assessed by projecting a line perpendicular to the width from the most anterior point of the incisive papilla (IP). The IP, RM, and LM points established the

bottom horizontal plane (BHP). The top horizontal plane (THP), which runs parallel to the BHP and is tangent to the highest point of the palate, was determined using Chebyshev's best-fit algorithm (see Fig. 3B). The palatal height was derived from the distance between the top and bottom horizontal planes (THP and BHP).

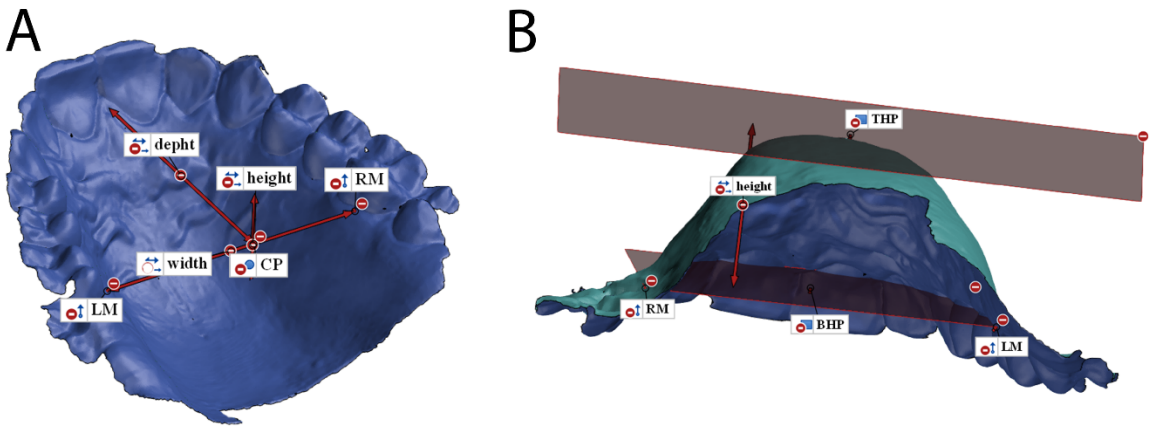

Fig. 3. Palatal vault geometry measurements. In picture A, the distance between the molars indicates the width of the palate, while the distance from the incisive papilla to the CP (central point) reflects the depth of the palate. In picture B, the measurement between the top horizontal plane (THP) and the bottom horizontal plane (BHP) illustrates the height of the palate. (RM: right first molar, LM: left first molar) (103)

3.2.2 Identification based on geometry

The differences in geometric parameters (i.e. height, depth and width) between the two scans were utilized to classify them as either 'identity' or 'stranger.' One participant was missing a first molar on both sides, while another had one missing on the left and one on the right, which affected a total of nine scans. Out of the 60 scans obtained from the remaining 20 participants, two scans were identified as defective. All scans were organized in MS EXCEL using a custom combination algorithm, with the order of items in the subset being irrelevant. This process resulted in 57 identity pairs and 1,596 stranger pairs. Initially, the absolute differences between the geometric parameters in the current validation dataset were computed and square-rooted to normalize the distribution (sqrd_height, sqrd_depth, and sqrd_width). These three square-rooted parameter differences were then incorporated into the two Fisher's linear discriminant functions that had been previously developed and published using the training set. (11). The mathematical formula that was used for the linear discriminant function is as follows:

$$Y_{identity} = 1.01 \times sqrd\_height + 1.00 \times sqrd\_width + 1.73 \times sqrd\_depth - 2.46.$$

$$Y_{stranger} = 3.59 \times sqrd\_height + 3.27 \times sqrd\_width + 3.65 \times sqrd\_depth - 9.23.$$

In the above formula, 'sqrd' represents the square root of the difference between the values measured for the two subjects being compared.
A higher Y score signifies the predicted category, distinguishing between 'identity' and 'stranger'.

The coefficients for Fisher's linear discriminant functions were established earlier (11) through the Linear Discriminant Analysis (LDA) method within the SPSS statistical software (V28, IBM, USA). The training set consisted of a single Caucasian population comprising 118 subjects, resulting in three scan repetitions and a total of 62,481 combinations of scan pairs (11).

3.2.3 Identification based on scan superimposition

Initially, both scans were loaded into the GOM Inspect® engineering analysis software (Suite 2020, GOM GmbH, Braunschweig, Germany). The scans were cropped to focus solely on the incisive papilla and the palatal rugae region. Afterwards, the comparison

between the two scans was conducted by superimposing them, where best-fit alignment was applied using the iterative closest point algorithm. This algorithm aimed to minimize the total distance by positioning the surface points of the scans as closely as possible. Similarly, as it is defined in the study 1, the minimized distance is represented by the MAD.

For the within-subject comparison (e.g., repeatability), two replicate scans of the same individual were aligned. For each participant, three comparisons were made:

1. scan1-scan2
2. scan1-scan3
3. scan2-scan3

For the between-subjects comparison, one scan from each participant was matched with the scans of the other 22 participants. Of the 69 scans, one of the three subjects was not of acceptable quality. As a result, 66 aligned pairs were considered for the repeatability assessment. Additionally, one alignment between two subjects was unsuccessful, despite being manually enforced. Consequently, 253 pairs were utilized for the between-subjects analysis. The alignment algorithm in the GOM Inspect® software provides three options to choose from: short, normal, and long, with a preference for the fastest outcomes. In the repeatability tests, the alignment was generally completed in the shortest time, while in the between-subjects group, the software required more time to align the two distinct scans with different anatomical features.

The variation between the aligned scans was evaluated by determining the MAD, the ratio of the integrated absolute distance between the aligned surfaces, and the area of the measured surfaces.

3.2.4 Sex determination based on geometry

Fisher's linear discriminant functions for determining sex were previously established using a population of Caucasian twins (11). The next two functions calculate the discrimination scores for females and males. The mathematical formula that was used for the linear discriminant function is as follows:

$$Y_{female} = 6.45 \times height + 5.56 \times width + 4.23 \times depth - 204$$

$$Y_{male} = 7.35 \times height + 5.91 \times width + 4.33 \times depth - 233$$

The higher score indicates the predicted sex. These functions were implemented as they are on the current population to assess their reliability and applicability.

3.2.5 Statistical analysis

In the geometric-based identification method, sensitivity, specificity, and accuracy were determined by tallying the correct and incorrect matches from a total of n = 1653 pairs. Logistic regression analysis was conducted to examine the connection between successful matches (the dependent outcome), the longitude and latitude of the country of origin (the independent covariate), and sex differences (the categorical independent variable).

In the superimposition-based identification method, a multiple linear regression analysis was performed using the between-subjects mean absolute distance (MAD) for n=253 as the dependent variable, with longitude, latitude, and sex serving as independent variables.

In the determination of sex, the sensitivity, specificity, and accuracy were assessed by evaluating the correct and incorrect matches among n=58 pairs.

A multiple linear regression analysis was conducted to examine the relationships between height, width, and depth as dependent variables and longitude, latitude, and sex as independent variables.

The sensitivity, specificity, and accuracy were reported along with their 95% confidence intervals (95% CI). The test set's results for sensitivity and specificity were compared to those of the training set using chi-square statistics. A p-value of less than 0.05 was considered statistically significant. All statistical analyses were performed using SPSS (Version 28, IBM, USA).

4 RESULTS

4.1 Study 1: *„Reproducibility of the digital palate in forensic investigations: a two-year retrospective cohort study on twins"*

4.1.1 The effect of orthodontic treatment and the comparison area on forensic reproducibility

In three instances, the physical impression was imperfect, leading to the exclusion of their indirect digitization data from the analysis. Of the participants, seventeen were involved in non-surgical orthodontic treatment that began either before 2019 or between 2019 and 2021. However, no significant difference ($p=0.777$) was found between the groups that received orthodontic treatment and those that did not (see Table 2 and Fig. 4).

Additionally, there were no significant interactions between orthodontic treatment and comparison area ($p=0.805$), between orthodontic treatment and scanning method ($p=0.158$), or among orthodontic treatment, comparison area, and scanning method ($p=0.856$). Conversely, measurements of the anterior palatal region exhibited significantly better repeatability ($p<0.001$) and technical reproducibility across all combinations (E_EA, E_ESB, E_PS, E_LAB, E_GYPS). As a result, the anterior area was utilized without differentiation regarding orthodontic treatment for subsequent analyses.

Table 2. Comparison of the Mean Absolute Distance (MAD) (in mm) between groups with orthodontic treatment and those without, as well as across aligned areas and scanning methods. (27)

E: Emerald scanner, ESA: Emerald S scanner with software version 'A', ESB: Emerald scanner with software version 'B', PS: Primescan, GYPS: gypsum model, LAB: laboratory scanner (27)

	Orthodontic treatment	Non-treated		Treated	
Scan pairs	Aligned area	Anterior	Complete	Anterior	Complete
E_E	Valid N	23	23	17	17
	Mean	0.023	0.040	0.021	0.034
	Standard Deviation	0.008	0.016	0.005	0.012
	Standard Error of Mean	0.002	0.003	0.001	0.003
E_ESA	Valid N	23	23	17	17
	Mean	0.081	0.107	0.071	0.102
	Standard Deviation	0.039	0.034	0.024	0.039
	Standard Error of Mean	0.008	0.007	0.006	0.009
E_ESB	Valid N	23	23	17	17
	Mean	0.081	0.110	0.067	0.098
	Standard Deviation	0.039	0.034	0.019	0.031
	Standard Error of Mean	0.008	0.007	0.005	0.007
E_GYPS	Valid N	21	21	16	16
	Mean	0.116	0.135	0.116	0.136
	Standard Deviation	0.045	0.051	0.043	0.048
	Standard Error of Mean	0.010	0.011	0.011	0.012
E_LAB	Valid N	21	21	16	16
	Mean	0.112	0.132	0.112	0.129
	Standard Deviation	0.045	0.054	0.042	0.046
	Standard Error of Mean	0.010	0.012	0.010	0.011
E_PS	Valid N	23	23	17	17
	Mean	0.080	0.095	0.072	0.096
	Standard Deviation	0.043	0.032	0.016	0.024
	Standard Error of Mean	0.009	0.007	0.004	0.006

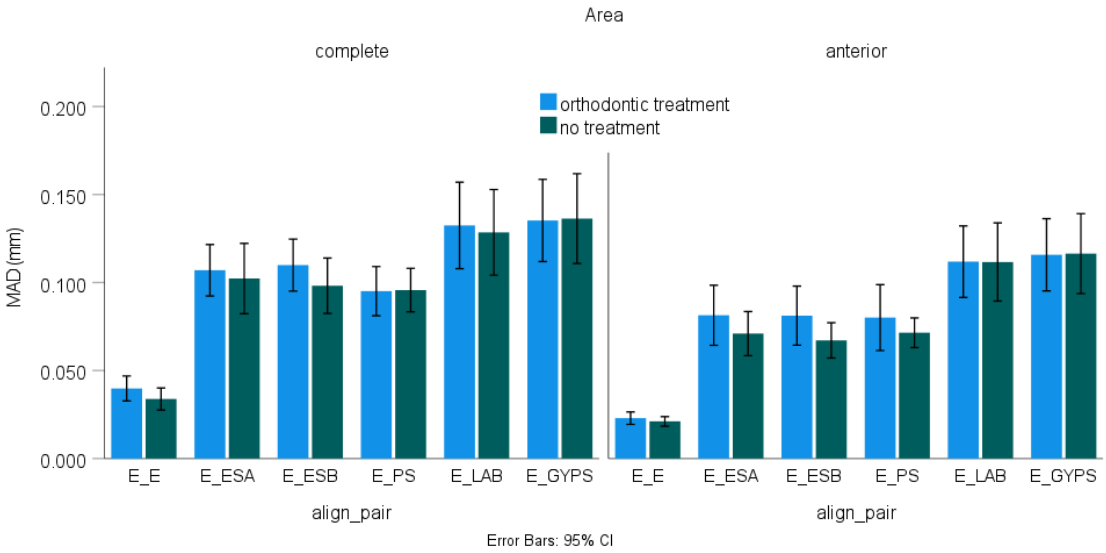

Fig. 4. The impact of orthodontic treatment and the aligned palatal region on forensic reproducibility, employing different scanning methods. E_E signifies repeatability, as all three replicate scans were conducted simultaneously using an Emerald intraoral scanner. In the designations E_E, E_ESA, E_ESB, E_PS, E_LAB, and E_GYPS (which relate to forensic reproducibility), the initial letter represents the first scan made by the Emerald scanner. Two years later, a second scan was performed using the Emerald S with various software versions, Primescan, or scanning of a physical impression or gypsum model. The bars illustrate the mean of the mean absolute distance (MAD) between the two scans following alignment, while the whiskers represent the 95% confidence intervals. (27)

4.1.2 The effect of the digitization method on forensic and technical reproducibility

The MAD values are presented in Table 3 and Figure 5. The technical reproducibility of the Emerald S across various software versions (ESB_ESA) did not show a significant difference when compared to the repeatability of the Emerald (E_E). In contrast, a comparison between the Emerald S and Primescan (ESA_PS) revealed lower technical reproducibility, although it was still higher than that of indirect digitization methods (ESA_LAB, ESA_GYPS). Overall, the results for technical reproducibility and repeatability were markedly better than those for forensic reproducibility. Given the inferior reproducibility of indirect digitization methods, only the IOS-based techniques were selected for further analysis.

Table 3. The mean absolute distance (MAD) (in mm) comparison of the repeatability, technical, and forensic reproducibility.

E: Emerald scanner, ESA: Emerald S scanner with software version 'A', ESB: Emerald scanner with software version 'B', PS: Primescan, GYPS: gypsum model, LAB: laboratory scanner, SD: Standard Deviation, SEM: Standard Error of Mean (27)

scan pairs	Valid N	Mean	SD	SEM	E_E	ESA_ESB	ESA_PS	ESA_LAB	ESA_GYPS	E_ESA	E_ESB	E_PS	E_LAB	E_GYPS
E_E	40	0.022	0.007	0.001		1.000	0.000	0.000	0.000	0.000	0.000	0.000	0.000	0.000
ESA_ESB	40	0.022	0.009	0.001	1.000		0.000	0.000	0.000	0.000	0.000	0.000	0.000	0.000
ESA_PS	40	0.037	0.012	0.002	0.000	0.000		0.000	0.000	0.000	0.000	0.000	0.000	0.000
ESA_LAB	37	0.089	0.050	0.008	0.000	0.000	0.000		1.000	0.829	0.499	0.780	0.029	0.006
ESA_GYPS	37	0.091	0.052	0.009	0.000	0.000	0.000	1.000		0.478	0.238	0.419	0.094	0.023
E_ESA	40	0.077	0.034	0.005	0.000	0.000	0.000	0.829	0.478		1.000	1.000	0.000	0.000
E_ESB	40	0.075	0.032	0.005	0.000	0.000	0.000	0.499	0.238	1.000		1.000	0.000	0.000
E_PS	40	0.076	0.034	0.005	0.000	0.000	0.000	0.780	0.419	1.000	1.000		0.000	0.000
E_LAB	37	0.112	0.043	0.007	0.000	0.000	0.000	0.029	0.094	0.000	0.000	0.000		1.000
E_GYPS	37	0.116	0.043	0.007	0.000	0.000	0.000	0.006	0.023	0.000	0.000	0.000	1.000	

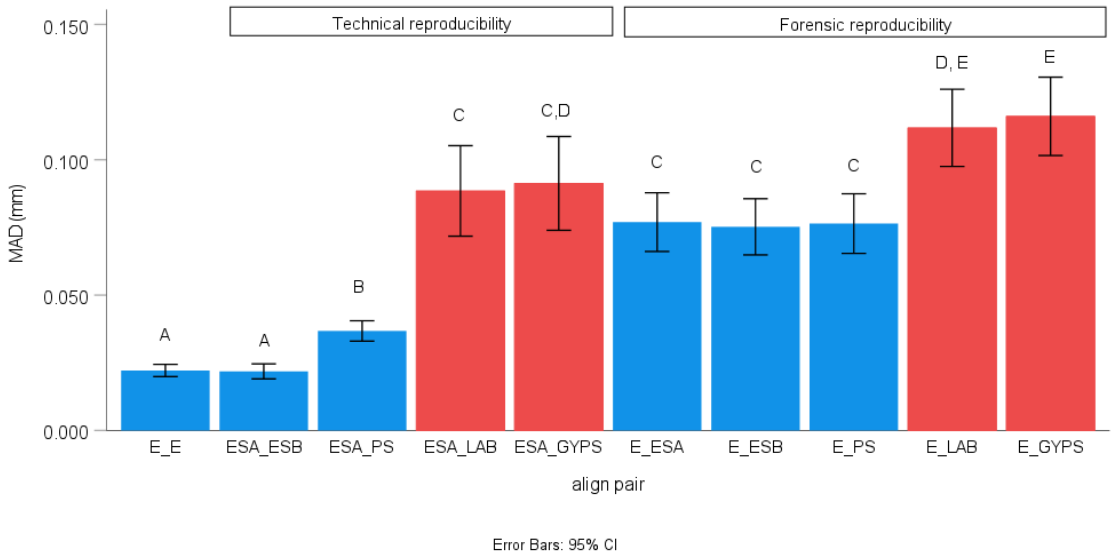

Fig. 5. Comparison of repeatability, technical, and forensic reproducibility. The first abbreviation (e.g. ESA) along the x-axis (alignment pair) represents the first scanner, while the second abbreviation denotes the second scanner used during alignment. E_E signifies repeatability (scans made by the Emerald scanner). The blue bars illustrate direct digitization through intraoral scanning (E: Emerald scanner, ESA: Emerald S scanner with software version 'A', ESB: Emerald S scanner with software version 'B', PS: Primescan), whereas the red bars represent indirect digitization from a physical impression (LAB) or a gypsum model (GYPS) by a laboratory scanner. Distinct capital letters above the bars highlight significant differences, with $p < 0.05$. (For example, 'A' is significantly different from 'B') The whiskers indicate the 95% confidence intervals (27).

4.1.3 Stability of the anterior palatal area over a two-year period

The median MAD in the anterior palatal region among monozygotic siblings was 0.343 mm (ranging from 0.252 to 0.525 mm) for the Emerald (E_E), 0.342 mm (with a range of 0.239 to 0.577 mm) for the Emerald S (ESA_ESA), and 0.377 mm (from 0.254 to 0.573 mm) for the Primescan (PS_PS). There were no significant differences in these values (p=0.575) (Fig. 6).

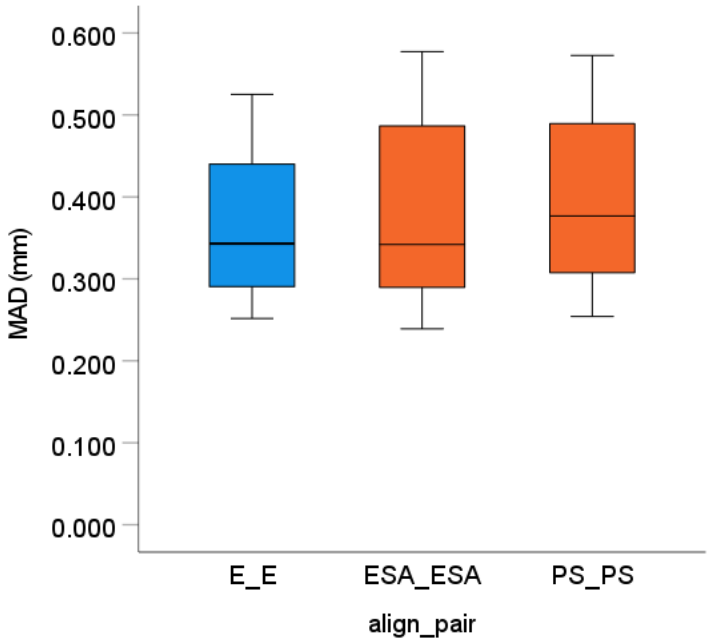

Fig. 6. The box and whisker plot illustrates the mean absolute distance (MAD) among siblings for the years 2019 (blue) and 2021 (orange). The scans of the twin siblings were conducted using identical scanners: Emerald in 2019 (E_E) and either Emerald S (ESA_ESA) or Primescan (PS_PS) in 2021. The lines that extend parallel from the boxes, known as whiskers, represent the minimum and maximum values. The box itself indicates the first and third quartiles. There was no significant difference found among the three medians. (27)

4.1.4 The discriminative potential of anterior palatal scans using an IOS

The scans from the 40 participants were matched with their duplicates obtained using the same scanner (E_E, repeatability), from different scanners at the same time (ESA_ESB, ESA_PS, technical reproducibility), and from different scanners at different times (E_ESA, E_ESB, E_PS, forensic reproducibility). A total of 240 alignment pairs were generated using IOSs, with 6 pairs for each participant. Additionally, 60 alignment pairs between siblings were created. The smallest mean absolute distance (MAD) between siblings was 0.239 mm (see Fig. 5). Using this as a benchmark, 237 out of the 240 replicates (98.8%) were accurately identified as belonging to the same individual. However, three forensic reproducibility values (E_ESA, E_ESB, E_PS) for one subject

overlapped with those of the sibling comparisons, resulting in a reduced classification rate. The maximum MAD recorded for reproducibility was 0.141 mm after removing three measurements from the same individual (refer to Fig. 7).

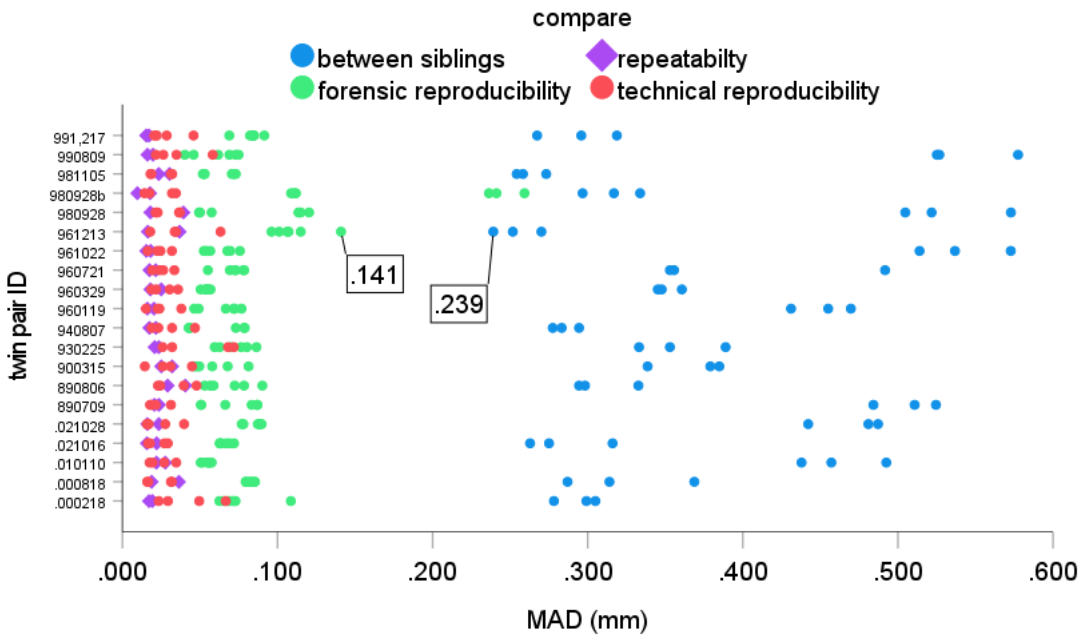

Fig. 7. The spreads in mean absolute distance (MAD) values observed within individuals using intraoral scanners. The values for repeatability (magenta dots), technical reproducibility (red dots), forensic reproducibility (green dots), and between-siblings mean absolute distance (MAD) (blue dots) are organized in rows for each twin pair. The data labels indicate the highest reproducibility value (0.141 mm, excluding the outlier) and the lowest between-siblings value (0.239 mm). The three green dots in the fourth row represent an outlier case where the forensic reproducibility values (E_ESA, E_ESB, E_PS) fell into the range of between-siblings values. (27)

Figure 8 presents a color-coded surface comparison map for a representative case from each group. Among the participants, one individual exhibited the highest forensic reproducibility values, having received orthodontic treatment during both the first and second sessions. On the left side, a palatally retained canine was moved to its place between 2019 and 2021 using an orthodontic appliance. The color-coded surface comparison map (Fig. 8D) highlighted a significant deviation between surfaces in the area of the upper left canine, and there were also alterations in the palatal vault (27).

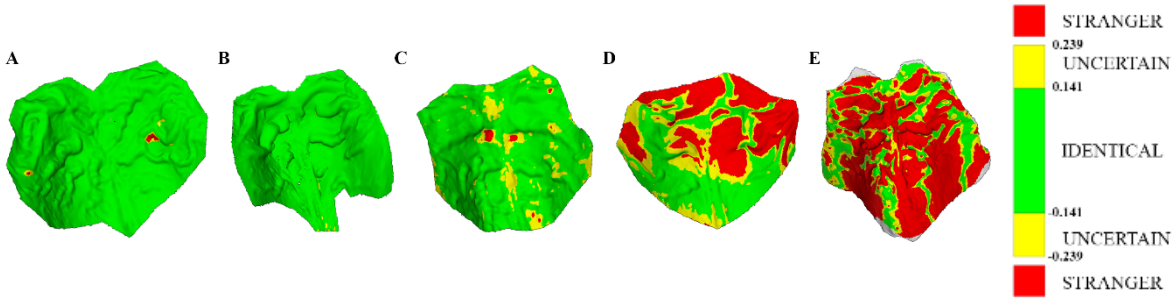

Fig. 8. Color-coded maps representing cases chosen from each comparison. (A) repeatability (E_E), (B) technical reproducibility (ESA_PS), (C) forensic reproducibility (E_ESA), (D) the canine case excluded from the forensic reproducibility comparison (E_ESA), and (E) comparisons between siblings (PS_PS). A cutoff value of 0.141 was established to distinguish between the identical range (green) and the uncertain range (yellow). Additionally, a second cutoff value of 0.239 was set to differentiate the uncertain range from the stranger range (red). (27)

4.2 Study 2: *„Human identification via digital palatal scans: a machine learning validation pilot study"*

4.2.1 Identification based on palatal geometry

The previously described (11) linear discriminant function, utilizing the variables of height, depth, and width measured within the currently used population, was able to differentiate between known individuals and strangers with a sensitivity of 91.2% (95% CI: 0.800-0.967%) and a specificity of 97.1% (95% CI: 0.961-0.978%). Chi-square statistics indicated that these values were not significantly different from the sensitivity of 91.2% (95% CI: 0.877-0.939%, $p = 0.99$) and specificity of 97.8% (95% CI: 0.976-0.979%, $p = 0.058$) observed in the homogeneous Caucasian population (10). The overall accuracy was recorded at 97.1% (95% CI: 96.12-97.82%).

Logistic regression showed that latitude (odds ratio = 1.010, $p = 0.735$) and longitude (odds ratio = 1.000, $p = 0.972$) had no impact on the number of accurate matches. However, when the palatal pairs being compared came from strangers of the opposite sex, the prediction rate increased by a factor of 5.4 (odds ratio = 5.4, $p < 0.001$).

4.2.2 Identification based on scan superimposition

Examples of intra- and between-subject superimposition are shown in Fig. 9.

The variability between subjects (1.068 - 0.214 mm) did not intersect with the repeatability range (0.011 - 0.093 mm) as shown in Table 4 and Figure 10. The differences in sex did not have a significant impact on the mean absolute distance (MAD) in the multiple linear regression analysis (partial correlation = -0.06, $p = 0.343$). Longitude difference exhibited a weak negative correlation with MAD (partial correlation = -0.16, $p < 0.01$), while latitude difference displayed a weak correlation that approached significance (partial correlation = -0.12, $p = 0.058$).

While neither ethnicity nor sex affected geometric discrimination or the precision of superimposition identification, height showed a significant correlation with latitude (partial correlation = 0.59, $p < 0.001$), longitude (partial correlation = -0.46, $p < 0.001$), and sex (partial correlation = 0.71, $p < 0.001$). Depth was significantly related to longitude (partial correlation = -0.32, $p < 0.05$) and sex (partial correlation = 0.31, $p < 0.05$), but not to latitude (partial correlation = -0.13, $p = 0.332$). Additionally, width was significantly affected by sex ($r = 0.38$, $p < 0.01$), while latitude (partial correlation = 0.18, $p = 0.174$) and longitude (partial correlation = 0.21, $p = 0.117$) did not exhibit significant influence.

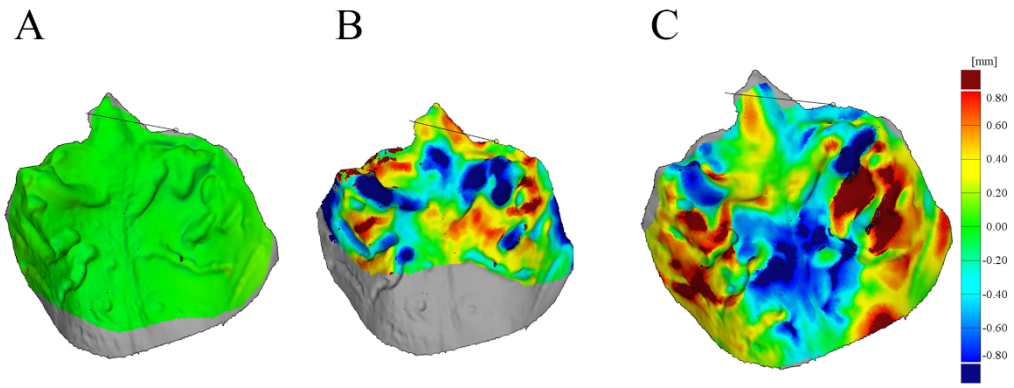

Fig. 9. Heat maps displaying the superimposition of scans for selected cases. The color coding illustrates the variation between the two scans within a range of −800 microns to +800 microns, indicating both positive and negative directions. Green signifies values that are approximately zero, while deeper shades of red or blue represent a larger distance between the two scans in that specific area. Yellow falls within the

intermediate range. The grey regions depict areas that were not captured in one of the scans. (A) The color map presents the overlap of two repeated scans from a female of Turkish descent. (B) The superimposed image features a Turkish female alongside a male of Chinese ancestry. (C) This comparison highlights the overlay of scans from two different Turkish females (103).

Table 4. The intra- (repeatability) and between-subjects mean absolute deviation (in mm)

CI: 95% confidence interval, Q1: first quartile, Q3: third quartile, Min: the lowest values, Max: the highest values (103)

	Mean	CI lower	CI upper	Median	Q1	Q3	Min	Max
repeatability	0.029	0.025	0.033	0.025	0.010	0.040	0.011	0.093
between-subjects	0.476	0.460	0.493	0.457	0.309	0.605	0.214	1.068

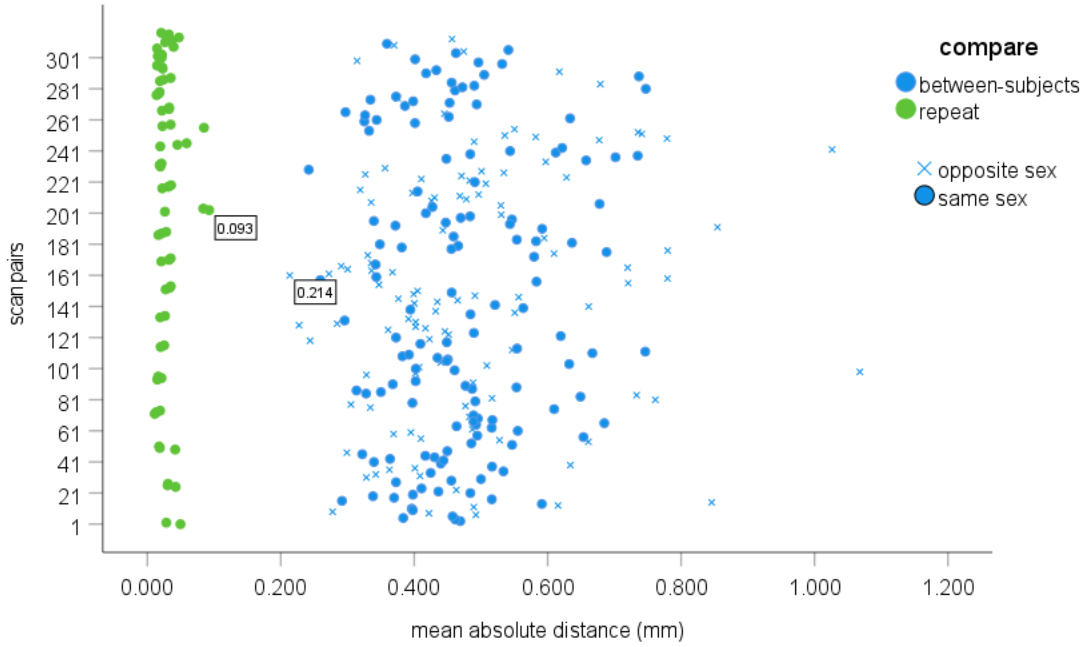

Fig. 10. Scatterplot of the mean absolute distance (MAD) among subjects. Green dots represent the repeatability, while the blue color indicates the mean absolute deviation (MAD) between subjects. A blue dot indicates alignment among subjects of the same sex, whereas a blue cross indicates alignment between subjects of different sexes. The label on the box highlights the highest repeatability and the lowest mean absolute deviation between subjects. (103)

While ethnicity and sex did not impact geometric discrimination or the accuracy of superimposition identification, height showed a substantial correlation with latitude (partial correlation = 0.59, $p < 0.001$), longitude (partial correlation = -0.46, $p < 0.001$), and sex (partial correlation = 0.71, $p < 0.001$). Conversely, depth was significantly influenced by longitude (partial correlation = -0.32, $p < 0.05$) and sex (partial correlation = 0.31, $p < 0.05$), but not by latitude (partial correlation = -0.13, $p = 0.332$). Width was notably affected by sex ($r = 0.38$, $p < 0.01$), but showed no significant correlation with latitude (partial correlation = 0.18, $p = 0.174$) or longitude (partial correlation = 0.21, $p = 0.117$).

4.2.3 Sex determination based on geometry

The above mentioned linear discriminative function, utilizing the variables measured within the current population, identified females more accurately than males, achieving a sensitivity of 69.0% (95% CI: 0.53-0.82%), which was not significantly lower ($p = 0.089$) than the homogenous Caucasian group, which had a sensitivity of 82.2% (95% CI: 0.72-0.89%) (10). In contrast, the specificity for the current population was 62.5% (95% CI: 0.36-0.84%), significantly lower ($p < 0.05$) than that of the homogenous population, which had a specificity of 89.3% (95% CI: 0.71-0.97%). The overall accuracy was 67.24% (95% CI: 53.66-78.99%).

5 DISCUSSION

Identifying the victims of a mass disaster is often challenging (1). Although there are established methods for identification, such as DNA analysis and fingerprinting, these techniques are not universally applicable due to the potential absence of reference (antemortem) data (9, 10). However, it should be noted that most patients have some form of dental records available. Consequently, dental identification is frequently the sole means of distinguishing dead bodies or human remains (2, 107). The introduction of digital technology in dentistry has led to the development of new tools, such as intraoral scanners. A significant number of dentists are shifting from conventional impression techniques to digital scanning methods (108), thereby facilitating greater accessibility to digital antemortem data.

A large number of studies have characterized the anterior portion of the palate, especially the palatal rugae, as exhibiting distinct and persistent patterns that change minimally over time. Studies have shown that the palate and palatal rugae can be used for human identification. Simon et al. conducted a study comparing the palatal morphology of over 200 twins. They found that intraoral scanners could differentiate between monozygotic twins (65). We aimed to reproduce these results using a subset of the same subjects (used in the previous investigation) under more challenging conditions. The subjects were two years older, some had undergone orthodontic treatment, and the palate was scanned using different methods in the second session. We aimed to see if the previously described identification method can still be applied. Furthermore, the objective was to determine whether orthodontic treatment affects the procedure.

In addition, an investigation was conducted to determine the applicability of the previously mentioned methodology to a cohort of individuals exhibiting diverse ethnic characteristics. We aimed to evaluate whether the identification method based on palatal morphology can be reliably used in a set of subjects coming from different ethnic backgrounds. For this purpose, an external validation study of the previously developed machine learning algorithm was conducted using 23 subjects from 11 different countries. Both a geometric-based and a superimposition-based identification method were completed. Both methods demonstrated reliability unaffected by the population employed.

- The 1st null hypothesis was accepted, as orthodontic treatment did not influence forensic reproducibility in our study.
- The 2nd null hypothesis was rejected, as the selection of the anterior area significantly increased forensic reproducibility.
- The 3rd null hypothesis was rejected, as the indirect digitization methods (both the impression and gypsum scanning) significantly decreased forensic reproducibility.
- The 4th null hypothesis of technical reproducibility was partially rejected, as the software version had no effect, whereas different IOS hardware resulted in significantly higher deviation.
- The 5th null hypothesis was accepted, as there was no change in the differences between MZ twins over two years in our study.
- The 6th null hypothesis was rejected, as the forensic reproducibility and the between-sibling difference were significantly different, and the spread of the data does not overlap.
- The 7th null hypothesis was accepted, as the accuracy of the palatal geometry-based discrimination algorithm remained unchanged in the ethnically heterogeneous population compared to the homogenous one.
- The 8th null hypothesis was accepted, as the accuracy of the superimposition-based discrimination algorithm remained unchanged in the ethnically heterogeneous population compared to the homogenous one.
- The 9th null hypothesis was rejected, as the accuracy of the sex determination significantly deteriorated in the ethnically heterogeneous population.

5.1 Different digitization methods and reproducibility

Our study indicates that the accuracy of palatal scans declines when an alternative digitization method is employed, as well as when scans are conducted two years apart. We refer to the alternative digitization method as technical reproducibility to differentiate it from the combined effects of aging and a different digitization method, which we label forensic reproducibility. Our study introduced these two new terms to the field of forensic literature.

The technical reproducibility and standard deviation of physical impressions and stone casts were 3-4 times worse than those of the intraoral scanners used in this study. Some impressions were discarded due to defects, such as bubbles or distortions. Moreover, physical impressions can compress soft tissues, whereas IOS does not (109). Consistent with this, previous research indicated that the reproducibility of segmented rugae on scans taken from a stone model exhibited a significant deviation of 178 µm (82). Another study has demonstrated that the accuracy of a palatal intraoral scan can match or even surpass that of a physical impression. (72). However, in that study, the impression was taken using a custom tray, whereas we utilized a plastic stock tray. Due to the shape of the palatal vault, the custom tray is the better choice. Nevertheless, it necessitates creating a stone model from an initial impression, which is impractical in postmortem scenarios. In cadaver studies, the time for investigation is restricted, and taking multiple physical impressions could harm the deteriorated tissue. Taneva et al. (69) evaluated the 3D variations in the medial and lateral endpoints of the rugae using two different indirect digitization techniques. They either digitized alginate impressions of the palate with the OrthoCAD™ system (Align Technology, Inc., San Jose, CA, USA) or scanned a plaster model using the Ortho Insight 3D™ desktop scanner (Motion View Software, LLC, Chattanooga, TN, USA). Their findings indicated that the only significant difference between the two methods was observed at the most posterior point of the incisive papilla, measuring 64 µm. The 12 endpoints of the first three rugae, however, did not show any significant discrepancies. Notably, when analyzing the digitized plaster model, there were no significant differences among individuals for the landmarks of the first and second rugae, but there were differences found in the third rugae. (69). The variability of individual values is more significant for discrimination purposes compared to the mean or median. In this analysis, the maximum reproducibility MAD values for the impression

and gypsum scans were recorded at 242 μm and 246 μm, respectively. Out of the 80 comparisons, 16 MAD values (20%) exceeded the minimum reproducibility threshold for forensic analysis of IOSs, which is set at 141 μm. In a similar study (81), the digitization of gypsum models demonstrated low reproducibility among individuals, with an average of 260 μm. Additionally, a comparison between digitized gypsum and intraoral scans during dentition analysis revealed lower reproducibility for indirect digitization, yielding a maximum value of 270 μm (66). In a dentate typodont model, the trueness of the complete arch scan was measured at 42 μm for Emerald, 22 μm for Emerald S, and 19 μm for Primescan (110). These trueness values are comparable to the trueness observed in the Planscanlab desktop scanner, which was reported at 28 μm in a recent study (79).

The indirect method is prone to extra errors stemming from the physical impression and gypsum modeling, which makes it inherently less reliable than direct techniques. As a result, indirect digitization may not be a dependable approach for superimposition-based identification.

Unlike indirect digitization, the IOS retains its ability to distinguish features in a forensic context. Even the highest mean absolute distance (MAD) of 141 μm achieved with various IOSs is significantly lower than the lowest MAD of 239 μm found among siblings using the same scanners. Taneva et al. (69) reported no significant difference in the 3D endpoint deviation of rugae among 15 individuals evaluated with an intraoral scanner. It is important to highlight, however, that not all pairs of individuals were directly compared; instead, a scan of one randomly chosen individual was compared to the others. Additionally, the differences in landmark coordinates varied from -248 μm to 151 μm, suggesting that signed values were utilized, which is an important distinction from measurements based on absolute values. The variations in landmark coordinates between individuals could potentially offset each other in three-dimensional space.

Bjelopavlovic et al. (56) acquired scans of the palates of 105 unrelated individuals using an Omnicam (Dentsply-Sirona, U.S.) intraoral scanner, repeating the process three months later. Following a 3D alignment of the two scans from the same person, the mean squared distance was calculated. Additionally, 105 comparisons between different subjects were randomly chosen from all possible pairings. The authors established a cut-off point of 300 μm to distinguish between individuals and strangers, which is greater than the minimum value observed between twin siblings (239 μm). This difference is

expected since monozygotic twins tend to resemble each other more closely than two unrelated individuals. While two randomly chosen subjects may appear similar by chance, it's unclear how many individuals would need to be selected to identify the smallest difference. Consequently, measurements from monozygotic twins are more appropriate for determining the cut-off point. Furthermore, the variation between twin siblings could be attributed to the fact that the morphology of palatal rugae is only partially influenced by genetic factors (57).

As a result, it is feasible to differentiate between identical twins through palatal assessment, rather than relying on the more demanding DNA analysis (111).

The forensic reproducibility of the intraoral scanners (E_ESA, E_ESB, E_PS) exceeded their technical reproducibility by 38-40 µm. In contrast, the technical reproducibility (ESA_PS) was only 15 µm greater than the repeatability observed with Emerald (E_E) or Emerald S (ESA_ESB). These findings could indicate a notable biological change in the palate over two years or suggest that the trueness of the various scanners varied. If we assume that the difference in reproducibility is exclusively due to a biological change, then a biological alteration should be of 38-40 µm over two years. However, a cross-sectional study indicated that the variation between siblings increased by only 3 µm annually (65). In addition, the current retrospective study indicates that the between-siblings deviation was comparable in 2019, as measured by Emerald, and in 2021, as assessed by Emerald S and Primescan. This implies that there was no change in the palate over the two years. While it is possible that both siblings experienced a change in the same direction, this scenario is unlikely. Consequently, a more reasonable explanation is that the greater deviation in forensic reproducibility, as opposed to technical reproducibility and repeatability, can be attributed to variations in the scanning devices used.

Based on studies, the trueness of Emerald S and Primescan has been enhanced compared to earlier-generation intraoral scanners like Emerald (73, 112, 113). This might explain the differences observed in the 2019 and 2021 data. In the case of a maxillary cadaver, the trueness and the precision of the palatal scan were recorded at 72 µm and 12 µm for Primescan (73) and 87 µm and 151 µm for Emerald, respectively (112). In another cadaver study two years later, the trueness was found to be 57 µm for both the Emerald S and Primescan (113).

Another study (114) demonstrated that both Emerald S (with a trueness of 83 µm and precision of 11 µm) and Primescan (with a trueness of 50 µm and precision of 21 µm) are roughly twice as accurate in complete arch scans compared to Emerald (which has a trueness of 175 µm and a precision of 50 µm). These disparities may account for the significantly higher mean absolute distances (MAD) observed when aligning the Emerald scan with the Primescan scan (E_PS, 76 µm) or the Emerald S scan (E_ESA, 77 µm; E_ESB, 75 µm), in comparison to aligning the Emerald S scan with the Primescan scan (ESA_PS, 37 µm).

The 37 µm technical reproducibility underscores the precision achieved when capturing palates *in vivo* using various novel intraoral scanners. Furthermore, the forensic reproducibility of Emerald S across different software versions (6.3.2.12 compared to 6.3.1.6) was comparable. While software updates often enhance accuracy (110), it seems that the latest generation of intraoral scanners may have already achieved a level of hardware accuracy where minor software updates yield little impact. However, a limitation of this study was that it compared the most recent complete-arch intraoral scanners with an older model. Therefore, it is likely that future comparisons between antemortem and postmortem data obtained using new intraoral scanners will show improvement.

Our new discovery indicates that focusing on the anterior part of the palate — specifically the rugae —for feature comparison greatly improves precision compared to analyzing the entire hard palate. This is because there is limited detail on the posterior soft tissues, resulting in lower scanning precision in that area (115). Additionally, elevated deviation values were observed in some cases for the lateral area around the molars (data not included in this thesis). This could be attributed to variations in the mucosal surface caused by the pulsing of the greater palatal artery. Moreover, a key benefit of concentrating on the anterior region is that it is often part of complete arch scans, even when making fixed dental prostheses.

5.2 The potential impact of orthodontic treatment

Our study found that orthodontic treatment did not influence the average forensic reproducibility. In another study (69), researchers observed no significant differences in

3D rugae landmarks 20 months post-orthodontic treatment, regardless of whether indirect or direct (iTero) digitization methods were employed, as long as the same method was consistently used before and after treatment. It is important to note that among the 15 subjects, five had undergone tooth extractions. Similarly, our findings indicated that orthodontic treatment did not impact the median values of 3D comparisons. However, we did experience a failure to identify an individual after orthodontic traction of a palatally retained canine. A prior study (11) demonstrated that the geometry of the palate is the primary factor influencing the alignment of two scans. A thorough examination of that specific case hinted at an alteration in palatal geometry.

In a prospective study, both extraction and non-extraction orthodontic treatments increased the average deviation between palatal scans; however, this did not hinder the ability to identify individuals (82). Additionally, it is proposed that orthodontic treatments involving tooth extraction or rapid maxillary expansion may alter the morphology of the rugae (41, 42, 82, 106). The accuracy of identifying individuals based on rugae patterns attenuated following orthodontic treatment that did not involve extractions (116, 117). However, the method was still suitable for identification purposes (116, 117). Another study revealed that while orthodontic treatment might influence the rugae patterns, the uniqueness of those patterns remains unchanged (36). As a result, in certain instances, extraction could affect the ability to distinguish between patterns.

5.3 Identification based on palatal geometry and by superimposition of digital scans

Our findings indicate that digital forensic analysis of the palatal vault is a practical, quick, and precise method for human identification, unaffected by population constraints. The palatal geometry-based approach exhibited a sensitivity of 91.2% and a specificity of 97.1% in the validation population from various countries. Interestingly, these results displayed a striking resemblance (with no overlap in confidence intervals) to the figures (91.2% and 97.8%) derived from the training set using a homogeneous Caucasian group (11). In summary, the previously suggested discriminant function remained similarly effective when applied to a varied mixed population.

In a similar vein, the superimposition method showed only minor variations, with the smallest between-subjects deviation of 214 μm and the highest repeatability of 93 μm in

the current mixed population. These data were strikingly similar to those found in the earlier study of the Caucasian population, which recorded 208 μm and 106 μm, respectively (65). Interestingly, the earlier study established the lower threshold for between-subject differences based on the variations observed between monozygotic twin siblings, which is anticipated to be less than the differences found between two unrelated individuals.

Therefore, the methods of superimposition and geometric identification showed reliable results across various populations, regardless of race or sex, suggesting that they can be applied broadly.

Taneva et al. (69) reported that both the indirect method (gypsum model scan) and the direct method (intraoral scan) are effective in differentiating individuals according to the superimposition technique within the U.S. population. They assessed the deviation of the rugae's endpoints and established threshold values ranging from 23 to 97 μm for identical subjects and from 15 to 248 μm for unrelated individuals.

Gibelli et al. (81) employed scanned gypsum models for superimposing palates. They established a threshold value of 500 μm to differentiate between individuals and strangers. This elevated threshold may be attributed to the indirect digitization technique used. In accordance with this, a recent study (27) suggested that the limitations of indirect digitization could hinder accurate identification. Initially, obtaining a flawless palatal impression without any bubbles proves to be difficult. Additionally, the additional procedures involved, such as producing a gypsum cast and performing laboratory digitization, contribute to overall errors. Moreover, the IOS is faster and more efficient when used at a disaster site and does not damage compromised tissue.

In another study (56), the IOS was employed to differentiate between unfamiliar subjects and identical scans. The threshold set for this discrimination was lower (300 μm) compared to that utilized in the study involving indirect digitization (81). However, this figure was still higher than what was observed in the current study (218 μm). Additionally, in certain instances, the difference between identical twin siblings reached as low as 208 μm (65). The 300 μm measurement could be associated with the previous version of the IOS, the Omnicam (Dentsply Sirona)(56). Nevertheless, the graphical representation in that paper showed that the intra-subject repeat was under 100 μm. As a result, their choice of an overly high cut-off value was likely too cautious.

5.4 Sex determination based on palatal geometry and superimposition of digital scans

The differences in sex among subjects did not enhance the effectiveness of the superimposition technique, and the participants' country of origin had only a slight impact. As a result, the superimposition method appears ineffective for determining sex. However, the geometric-based sex discrimination function demonstrated lower sensitivity and specificity (69.0% and 62.5%, respectively) in a diverse population compared to a more homogeneous one, which showed sensitivity at 82.2% and specificity at 89.3% (11). This is most likely attributable to genetic variations among different populations.

Interestingly, the data from the current study revealed that males exhibited a lower match (specificity) compared to females (sensitivity). In contrast, the training set indicated the reverse, with males showing a higher match (specificity) than females. Additionally, height demonstrated the greatest potential for discrimination within Fisher's Linear Discriminant function (11) and was strongly correlated with sex. In this mixed ethnic population, the standard deviations for height, depth, and width were recorded as 1.1, 2.6, and 2.5 mm for females, while males had values of 3.1, 3.6, and 2.4 mm, respectively. The significant reduction in height variability (standard deviation) for females—being three times less than that of males—might contribute to a heightened sensitivity in identifying them. However, it's worth noting that in the previous training set, the height standard deviations between sexes were somewhat different. The function derived from the training set was subsequently applied to the test set without any adjustments. As a result, the differences in height standard deviations across the populations could explain the attenuated sensitivity observed in the current findings.

Additionally, males exhibited a larger palate than females in the Hungarian population (11), in the Lebanese population (118), and in India (119). The height in our study was notably affected by latitude and longitude, indicating an interactive influence of sex and population on height. As a result, the differences among populations may hinder precise sex determination.

5.5 An implication for ethnic differentiation based on palatal geometry

In cases where the antemortem scan database is not available during mass disaster scenarios, variations in palatal morphology due to ethnic differences can be crucial to advancing forensic investigation by pointing to the country of origin, where antemortem data should be sought.

Although the morphological distinctions between distant populations, like Chinese and Caucasians, are apparent, the differences among closer groups, such as Germans and Greeks or Persians and Iraqis, are less noticeable. We proposed that the geographic distance between countries of origin offers a more reliable measure (quantified on a continuous scale) compared to subjective categories like Black, Caucasian, Arabic, Indian, or Asian.

Our findings showed that identification using either approach is not influenced by the individual's country of origin, indicating that the specific individual is the main factor in determining the palatal vault. In contrast, sex, latitude, and longitude had a moderate impact on both height and depth measurements. As a result, individuals from northern and western regions tend to have a higher palate compared to those from southern and eastern regions, with western individuals also displaying a somewhat deeper palate than their eastern counterparts.

The more significant relationship between sex and geometric measurements, in comparison to latitude and longitude, indicates that ethnicity cannot be accurately inferred without first establishing the individual's sex. Consequently, it is essential to conduct a large-scale study that ensures a well-balanced ratio of males and females across different countries. Given our current findings, this type of research could lead to the creation of a generalized discriminant function for predicting ethnicity. Our pilot study could help initiate international collaboration toward this goal.

5.6 Strengths and limitations

The strength lies in the fact that the validation of the geometric and superimposition-based identification and sex determination method was conducted in an unexpected context, without any intention to influence participant inclusion or exclusion. As a result, the countries of origin and the distribution of sexes were coincidental. This random distribution may explain why the accuracy of sex determination was notably lower than

what has been observed in larger subsets in the past. Therefore, it's essential to develop new classification functions for sex determination using a comprehensive training dataset that deliberately includes participants from various geographic regions, ensuring a balanced representation of both males and females.

In terms of forensic purposes, a limitation might be the possible absence of digital technology. Although fewer and fewer dental practices still rely on traditional physical impressions, issues such as the inconsistent reproduction of the palate on gypsum models, along with insufficient storage for physical models, could hinder access to antemortem data. However, this will probably change in the near future. Surveys conducted in 2020 (68) indicated that 50% of dental practices in the U.S. already possess an intraoral scanner. A more recent study from 2023 found that in the examined countries, more than 75% of dental professionals use an intraoral scanner on a daily basis (108).

Another limitation is that, in restorations involving one or three teeth, only one quadrant is often examined. As a result, the antemortem scan might capture only half of the dental arch, and the postmortem scan could be impaired on the same side, complicating the matching process. Recent findings indicate that the palate exhibits significant symmetry along the sagittal plane (105). Nonetheless, the shape of the rugae and the general contour of the vault show marked differences between the two sides (120), making it often impossible to use the opposite side for comparison.

The geometric identification method proved to be highly effective in unforeseen forensic situations. However, analysis could only be conducted on 87% of the participants, as three individuals were missing at least one maxillary first molar, which rendered distance measurements unfeasible. In the earlier stages of developing the identification algorithm, it should have been noted that a slightly higher percentage (16%) would need to be excluded due to the absence of first molars (11). The presence of specific older individuals could account for this. The proportion of missing molars in the comprehensive forensic dental database Odontosearch aligns with our findings (15). In contrast, the superimposition-based technique can be effectively used in situations where the palatal geometry is indeterminate. However, this method does come with the drawback of being slower and requiring more computational resources. In the absence of automated software, the need for manual alignment restricts the evaluation of between-subject comparisons in research, especially as the sample size increases; the potential

number of pairs or combinations can escalate rapidly, following a quadratic pattern. Consequently, researchers often create a subset by randomly choosing pairs from the total possible combinations (56, 81).

Although dental records, fingerprints, and DNA are still the main methods of identification (121, 122), intraoral scanners have started to be recognized as a promising tool for human identification by analyzing dental morphology and the anterior palate (11, 56, 66, 69, 81, 83-85, 123). Digital records enable quicker searches within databases, and a statistically driven comparison algorithm not only yields straightforward match or no-match results but also assigns a probability to each outcome (86), thereby increasing the reliability of identification. However, this approach should not be viewed as the main method of identification. Rather, it serves to refine the antemortem data pool and supports other methods of identification. Considering the evident benefits of intraoral scanners, we recommend that they be regarded as a supplementary tool in forensic investigations, even though they have not yet been integrated into standard practices.

One design limitation of the first study is the relatively short follow-up time. Over a longer period, more changes to the rugae may occur. Further studies are needed to examine potential long-term changes to the palate and rugae. Another important limitation of the first study is that the 2019 scanner was an older version of the 2021 scanner. In real-life forensic scenarios, antemortem and postmortem scans are often captured using different types of scanners. In our study, we aimed to simulate such a scenario. The difference in measured data may raise questions as to whether the differences in results are caused by the difference in scanners or by biological change. In the first study, the deviation between siblings was similar in 2019 when measured by the Emerald scanner, and in 2021 when measured by the Emerald S and Primescan. This suggests that there was no biological change in the palate over the two years.

A limitation of the second study is its small sample size and imbalanced distribution of sex and country of origin. However, the primary aim of the second study was to provide an external validation of the previously published machine learning algorithm on a test group. From the perspective of the secondary aim (i.e., evaluating the effect of the ethnic background), it can be considered a pilot study. Further studies are needed to examine the impact of palate dimensions, ethnic background and sex.

5.7 Future advancements and considerations

Further investigation is necessary to determine how long after death the palatal rugae-based identification method can be used. Currently, there is very little data on this topic (34). In an animal study of lambs, subjects could be identified using intraoral scanners up to five days after death; however, they could still provide valuable information up to 20 days postmortem (104).

Moreover, additional studies are needed to assess aging, particularly in patients with complete dentures, as well as the impact of palatal tissue harvesting for regenerative surgery.

The primary drawback of both superimposition and geometry-based techniques is the absence of a centralized database for antemortem intraoral scans. Nevertheless, recent efforts have been initiated to address this issue. For instance, Xiong et al. developed the largest dataset available so far, which includes 16,000 intraoral scans (124).

An effective database suitable for human identification in a mass disaster scenario would require a much larger database. While the likelihood of creating a database containing scans of everyone on the planet is slim, an incomplete database could still help identify matches between scans of the same individual.

In the future, by establishing a comprehensive global database of intraoral scans, ideally encompassing all individuals, this method could enable rapid and highly accurate identification without relying only on traditional biometric markers such as fingerprints or DNA. An automated algorithm capable of efficiently matching intraoral scans would streamline identification processes in various scenarios, from criminal investigations to emergency response.

Attempts have been made to develop automatic algorithms to find matches between scans of individuals (125, 126). Petersen et al. designed software using the Trimesh and Open3D Python libraries that can significantly speed up the identification process by automatically extracting palatal rugae from standard triangulation language (STL) files of the entire palate (19). Bjelopavlovic et al. also developed an automated 3D alignment algorithm with a 100% success rate in identifying matching palatal scans.(127)

Nonetheless, these methods bring up significant ethical concerns related to privacy, data security, and obtaining consent (128, 129). As technology advances, careful regulation and responsible data management will be essential to harness its benefits while

safeguarding individual rights. Ultimately, intraoral scan-based identification could revolutionize how we verify identity, offering a biometric solution that is both unique and resilient against forgery.

6 CONCLUSIONS

- The reproducibility of palatal scans obtained with different intraoral scanners is acceptable for human identification.
- The reproducibility remains acceptable after a two-year interval, regardless of the presence of non-surgical orthodontic treatment.
- Digitization of physical impressions made with stock trays or casts is unreliable for comparing palatal features.
- Intraoral scanning of the anterior palatal area (i.e., palatal rugae) demonstrates superior reproducibility, independent of the IOS brand.

- The palatal vault geometry- and the superimposition-based identification methods are good candidates for forensic feature comparison.
- The accuracy of machine learning based on palatal geometry is consistent across different populations.
- Sex can be determined from palatal geometry with moderate accuracy.

7 SUMMARY

Objectives: Previous studies suggest that the palate and palatal rugae can serve as individual markers in human identification. This thesis aimed to confirm the feasibility of a palate-based identification method, evaluate its applicability across different digitization techniques, and assess the influence of ethnic background.

Methods: The palate was scanned three times and two years later in 20 pairs of monozygotic twins (40 individuals) using intraoral scanners (IOS) to assess repeatability. Additionally, elastic impressions and plaster models were created and digitized with a laboratory scanner. The mean absolute distance (MAD) between scans was compared after best-fit alignment to evaluate forensic reproducibility. Comparisons across sessions assessed the effects of aging, orthodontic treatment, and digitization methods, while scans from different digitization techniques in the second session examined technical reproducibility. Sibling differences over time were analyzed to evaluate aging effects. In a second study, 23 individuals from 11 countries were scanned, and superimposition (MAD) and geometric dimensions (height, width, depth) were assessed.

Results: The anterior palatal area showed significantly better repeatability and forensic reproducibility than the entire palate ($p < 0.001$), with orthodontic treatment having no effect. Indirect digitization produced lower reproducibility than IOSs, with forensic MAD values of 75–77 µm and technical MAD of 37 µm. IOS scans demonstrated a repeatability of 22 µm, significantly better ($p < 0.001$). No significant differences emerged in sibling comparisons over time; the closest sibling MAD (239 µm) exceeded the highest forensic MAD (141 µm), indicating good discriminative capacity. The geometric evaluation achieved 91.2% sensitivity and 97.1% specificity. Latitude and longitude did not significantly affect geometric matches, and MAD ranges for superimposition (1.068–0.214 mm) and repeatability (0.011–0.093 mm) did not overlap. For sex determination, the method recognized females over males with 69.0% sensitivity and 62.5% specificity.

Conclusions: Reproducibility between different IOS devices remains acceptable over two years, though poor between IOS and indirect digitization. The anterior palate appears relatively stable in young adults. Geometric and superimposition methods demonstrated robust reliability, unaffected by population differences, whereas sex prediction showed only moderate accuracy.

8 REFERENCES

1. Caldas IM, Magalhães T, Afonso A. (2007) Establishing identity using cheiloscopy and palatoscopy. Forensic Sci Int, 165: 1-9.
2. Tin D, Cheng L, Le D, Hata R, Ciottone G. (2024) Natural disasters: a comprehensive study using EMDAT database 1995–2022. Public Health, 226: 255-260.
3. Petju M, Suteerayongprasert A, Thongpud R, Hassiri K. (2007) Importance of dental records for victim identification following the Indian Ocean tsunami disaster in Thailand. Public Health, 121: 251-257.
4. Tsokos M, Lessig R, Grundmann C, Benthaus S, Peschel O. (2006) Experiences in tsunami victim identification. Int J Legal Med, 120: 185-187.
5. Morgan OW, Sribanditmongkol P, Perera C, Sulasmi Y, Van Alphen D, Sondorp E. (2006) Mass fatality management following the South Asian tsunami disaster: case studies in Thailand, Indonesia, and Sri Lanka. PLoS Med, 3: e195.
6. Balikuddembe JK, Reinhardt JD, Vahid G, Di B. (2024) A scoping review of post-earthquake healthcare for vulnerable groups of the 2023 Turkey-Syria earthquakes. BMC Public Health, 24: 945.
7. Romanello M, Napoli Cd, Green C, Kennard H, Lampard P, Scamman D, Walawender M, Ali Z, Ameli N, Ayeb-Karlsson S, Beggs PJ, Belesova K, Berrang Ford L, Bowen K, Cai W, Callaghan M, Campbell-Lendrum D, Chambers J, Cross TJ, van Daalen KR, Dalin C, Dasandi N, Dasgupta S, Davies M, Dominguez-Salas P, Dubrow R, Ebi KL, Eckelman M, Ekins P, Freyberg C, Gasparyan O, Gordon-Strachan G, Graham H, Gunther SH, Hamilton I, Hang Y, Hänninen R, Hartinger S, He K, Heidecke J, Hess JJ, Hsu S-C, Jamart L, Jankin S, Jay O, Kelman I, Kiesewetter G, Kinney P, Kniveton D, Kouznetsov R, Larosa F, Lee JKW, Lemke B, Liu Y, Liu Z, Lott M, Lotto Batista M, Lowe R, Odhiambo Sewe M, Martinez-Urtaza J, Maslin M, McAllister L, McMichael C, Mi Z, Milner J, Minor K, Minx JC, Mohajeri N, Momen NC, Moradi-Lakeh M, Morrissey K, Munzert S, Murray KA, Neville T, Nilsson M, Obradovich N, O'Hare MB, Oliveira C, Oreszczyn T, Otto M, Owfi F, Pearman O, Pega F, Pershing A, Rabbaniha M, Rickman J, Robinson EJZ, Rocklöv J, Salas RN, Semenza JC,

Sherman JD, Shumake-Guillemot J, Silbert G, Sofiev M, Springmann M, Stowell JD, Tabatabaei M, Taylor J, Thompson R, Tonne C, Treskova M, Trinanes JA, Wagner F, Warnecke L, Whitcombe H, Winning M, Wyns A, Yglesias-González M, Zhang S, Zhang Y, Zhu Q, Gong P, Montgomery H, Costello A. (2023) The 2023 report of the Lancet Countdown on health and climate change: the imperative for a health-centred response in a world facing irreversible harms. The Lancet, 402: 2346-2394.

8. Interpol. (2023) Disaster Victim Identification (DVI) Guide https://www.interpol.int/en/How-we-work/Forensics/Disaster-Victim-Identification-DVI date of access: 17.01.2026.
9. Holdren JP, Lander ES. (2016) Forensic Science in Criminal Courts: Ensuring Scientific Validity of Feature-Comparison Methods (Governmental report) Executive Office of the President, President's Council of Advisors on Science and Technology, Forensic Science in Criminal Courts (USA) https://digitalcollections.rice.edu/Documents/Detail/forensic-science-in-criminal-courts-ensuring-scientific-validity-of-feature-comparison-methods/266483 date of access: 17.01.2026.
10. Willis AJ, Myers L. (2001) A cost-effective fingerprint recognition system for use with low-quality prints and damaged fingertips. Pattern Recognit, 34: 255-270.
11. Simon B, Aschheim K, Vag J. (2022) The discriminative potential of palatal geometric analysis for sex discrimination and human identification. J Forensic Sci, 67: 2334-2342.
12. Farronato M, Begnoni G, Boodt LD, Thevissen P, Willems G, Cadenas de Llano-Pérula M. (2023) Are palatal rugae reliable markers for 3D superimposition and forensic human identification after palatal expansion? A systematic review. Forensic Sci Int, 351: 111814.
13. de Boer HH, Roberts J, Delabarde T, Mundorff AZ, Blau S. (2020) Disaster victim identification operations with fragmented, burnt, or commingled remains: experience-based recommendations. Forensic Sci Res, 5: 191-201.
14. Charangowda BK. (2010) Dental records: An overview. J Forensic Dent Sci, 2: 5-10.

15. Adams BJ, Aschheim KW. (2016) Computerized Dental Comparison: A Critical Review of Dental Coding and Ranking Algorithms Used in Victim Identification. J Forensic Sci, 61: 76-86.
16. Ermenc B, Rener K. (1999) Possibilities for dental identification in the case of mass disaster in Slovenia. Forensic Sci Int, 103: S67-S75.
17. Sims CA, Berketa J, Higgins D. (2020) Is human identification by dental comparison a scientifically valid process? Sci Justice, 60: 403-405.
18. Simon B, Farid AA, Freedman G, Vag J. (2021) Digital scans and human identification. Oral Health Vol. July 9 pp. 36-39, Oral Health Group
19. Petersen A, Villesen P, Staun Larsen L. (2025) The Oral Fingerprint: Rapid comparison of palatal rugae for forensic identification. Front. Radiol.: 18:15:1638294.
20. Corrêa Silva-Sousa A, Carvalho C, Marañón-Vásquez G, Matsumoto M, Stuani M, Oliveira HM, Lepri C, Proff P, Paddenberg E, Kirschneck C, Kuchler E. (2021) Tooth agenesia might be associated with palatine rugae pattern in a tooth Brazilians population. Res., Soc. Dev., 10: e29010716487.
21. Roselli L, Mele F, Suriano C, Santoro V, Catanesi R, Petruzzi M. (2024) Palatal rugae assessment using plaster model and dental scan: a cross-sectional comparative analysis. Front Oral Health, 5: 1456377.
22. Trakanant S, Nihara J, Kawasaki M, Meguro F, Yamada A, Kawasaki K, Saito I, Takeyasu M, Ohazama A. (2020) Molecular mechanisms in palatal rugae development. J Oral Biosci, 62: 30-35.
23. Amasaki H, Ogawa M, Nagasao J, Mutoh K-i, Ichihara N, Asari M, Shiota K. (2003) Distributional changes of BrdU, PCNA, E2F1 and PAL31 molecules in developing murine palatal rugae. Ann Anat, 185: 517-523.
24. BUCHTOVA M. (2003) The development of palatal rugae in the European pine vole, Microtus subterraneus (Arvicolidae, Rodentia). Folia Zoo, 52: 127-136.
25. Jain A, Chowdhary R. (2014) Palatal rugae and their role in forensic odontology. J Investig Clin Dent, 5: 171-178.
26. Kapali S, Townsend G, Richards L, Parish T. (1997) Palatal rugae patterns in Australian aborigines and Caucasians. Aust Dent J, 42: 129-133.

27. Mikolicz A, Simon B, Gaspar O, Shahbazi A, Vag J. (2023) Reproducibility of the digital palate in forensic investigations: a two-year retrospective cohort study on twins. J Dent, 135: 104562.
28. Simmons JD, Moore RN, Erickson LC. (1987) A longitudinal study of anteroposterior growth changes in the palatine rugae. J Dent Res, 66: 1512-1515.
29. Chong JA, Mohamed AMFS, Pau A. (2020) Morphological patterns of the palatal rugae: A review. J Oral Biosci, 62: 249-259.
30. Thomas CJ, van Wyk CW. (1988) The palatal rugae in an identification. J Forensic Odontostomatol, 6: 21-27.
31. Malekzadeh AR, Pakshir HR, Ajami S, Pakshir F. (2018) The Application of Palatal Rugae for Sex Discrimination in Forensic Medicine in a Selected Iranian Population. Iran J Med Sci, 43: 612-622.
32. Jain A, Chowdhary R. (2014) Palatal rugae and their role in forensic odontology. J Investig Clin Dent, 5: 171-178.
33. Hill AJ, Lain R, Hewson I. (2011) Preservation of dental evidence following exposure to high temperatures. Forensic Sci Int, 205: 40-43.
34. Muthusubramanian M, Limson KS, Julian R. (2005) Analysis of rugae in burn victims and cadavers to simulate rugae identification in cases of incineration and decomposition. J Forensic Odontostomatol, 23: 26-29.
35. Almeida MA, Phillips C, Kula K, Tulloch C. (1995) Stability of the palatal rugae as landmarks for analysis of dental casts. Angle Orthod, 65: 43-48.
36. Mustafa AG, Allouh MZ, Alshehab RM. (2015) Morphological changes in palatal rugae patterns following orthodontic treatment. J Forensic Leg Med, 31: 19-22.
37. Kratzsch H, Opitz C. (2000) Investigations on the palatal rugae pattern in cleft patients. Part I: A morphological analysis. J Orofac Orthop, 61: 305-317.
38. Gupta AA, Kheur S, Alshehri A, Awadh W, Ahmed ZH, Feroz SMA, Khan SS, Mushtaq S, Dewan H, Khurshid Z, Varadarajan S, Sujatha G, Veeraraghavan VP, Patil S. (2022) Is Palatal Rugae Pattern a Reliable Tool for Personal Identification following Orthodontic Treatment? A Systematic Review and Meta-Analysis. Diagnostics (Basel), 12.

39. Trizzino A, Messina P, Sciarra FM, Zerbo S, Argo A, Scardina GA. (2023) Palatal Rugae as a Discriminating Factor in Determining Sex: A New Method Applicable in Forensic Odontology? Dent J (Basel), 11.
40. Taylor PT, Wilson ME, Lyons TJ. (2002) Forensic odontology lessons: multishooting incident at Port Arthur, Tasmania. Forensic Sci Int, 130: 174-182.
41. Bailey LT, Esmailnejad A, Almeida MA. (1996) Stability of the palatal rugae as landmarks for analysis of dental casts in extraction and nonextraction cases. Angle Orthod, 66: 73-78.
42. Ali B, Shaikh A, Fida M. (2016) Stability of Palatal Rugae as a Forensic Marker in Orthodontically Treated Cases. J Forensic Sci, 61: 1351-1355.
43. Makrygiannakis MA, Konstantonis D, Vastardis H, Athanasiou AE, Halazonetis DJ. (2024) Palatal rugae change shape following orthodontic treatment: a comparison between extraction and non-extraction borderline cases using fractal analysis and 3D superimposition. Eur J Orthod, 47.
44. Ziar N, Pakshir HR, Alamdarloo Y, Ajami S. (2023) Characteristic changes of the palatal rugae following orthodontic treatment. Egypt J Forensic Sci, 13: 14.
45. Peavy DC, Jr., Kendrick GS. (1967) The effects of tooth movement on the palatine rugae. J Prosthet Den, 18: 536-542.
46. Bowles RG. (2005) First premolar extraction decisions and effects.
47. Camargo PM, Melnick PR, Kenney EB. (2001) The use of free gingival grafts for aesthetic purposes. Periodontol 2000, 27: 72-96.
48. Hoggan BR, Sadowsky C. (2001) The use of palatal rugae for the assessment of anteroposterior tooth movements. Am J Orthod Dentofacial Orthop, 119: 482-488.
49. Allen H. (1888) The Palatal Rugae in Man. Proceedings of the Academy of Natural Sciences of Philadelphia, 40: 254-272.
50. Shetty D, Juneja A, Jain A, Khanna KS, Pruthi N, Gupta A, Chowdhary M. (2013) Assessment of palatal rugae pattern and their reproducibility for application in forensic analysis. J Forensic Dent Sci, 5: 106-109.
51. Smitha T, Vaswani V, Deepak V, Sheethal HS, Hema KN, Jain VK. (2021) Reliability of palatal rugae patterns in individual identification. J Oral Maxillofac Pathol, 25: 555.

52. Bansode SC, Kulkarni MM. (2009) Importance of palatal rugae in individual identification. J Forensic Dent Sci, 1.
53. Palatinas R, de su Forma SdA. (2009) Palatal rugae: Systematic analysis of its shape and dimensions for use in human identification. Int. j. morphol, 27: 819-825.
54. Makrygiannakis MA, Vastardis H, Athanasiou AE, Halazonetis DJ. (2022) Novel method to delineate palatal rugae and assess their complexity using fractal analysis. Sci Rep, 12: 21749.
55. Khelkar P, Mangulkar AP, Sachdev SS, Karjodkar FR, Unnikrishnan A. (2025) Palatal rugae pattern and tongue print as a potential tool for gender identification in forensic odontology: a cross-sectional study. Bull. Int. Assoc. Paleodont., 19: 33-41.
56. Bjelopavlovic M, Degering D, Lehmann KM, Thiem DGE, Hardt J, Petrowski K. (2023) Forensic Identification: Dental Scan Data Sets of the Palatal Fold Pairs as an Individual Feature in a Longitudinal Cohort Study. Int J Environ Res Public Health, 20.
57. Chong JA, Syed Mohamed AMF, Marizan Nor M, Pau A. (2020) The Heritability of Palatal Rugae Morphology Among Siblings*†. J Forensic Sci, 65: 2000-2007.
58. Rojas-Torres JA, López-Lázaro S, Viciano J, Fonseca GM. (2025) Digital matching of palatal rugae patterns for forensic identification in edentulous denture wearers. Forensic Science, Medicine and Pathology, 21: 157-164.
59. Carbajo C, de Policía Científica B. (2015) Identificación de cadáveres y aspectos forenses de los desastres. Publicaciones de la Unidad de Investigación en Emergência y Desastres, 2: 12-25.
60. Emam ،NM. (2024) Role of Forensic Odontology in Identification of Persons: A Review Article. Cureus, 16: e56570.
61. Abdul NS, Alzahrani JA, Alharbei SS, Almutib AT, Ibnjuma RA, Almutairi ZH. (2024) Palatal Rugoscopy: A Tool for Ethnicity and Gender Identification Among Saudi and Kuwaiti Populations. Cureus, 16: e52333.
62. Gupta V, Kaur A. (2021) Palatal rugoscopy as an adjunct for sex determination in forensic odontology (Sri Ganganagar population): A cross-sectional study of 100 subjects. J Oral Maxillofac Pathol, 25: 556.

63. Kaul B, Vaid V, Gupta S, Kaul S. (2021) Forensic Odontological Parameters as Biometric Tool: A Review. Int J Clin Pediatr Dent, 14: 416-419.
64. Hemanth M, Vidya M, Shetty N, Karkera BV. (2010) Identification of individuals using palatal rugae: Computerized method. J Forensic Dent Sci, 2: 86-90.
65. Simon B, Liptak L, Liptak K, Tarnoki AD, Tarnoki DL, Melicher D, Vag J. (2020) Application of intraoral scanner to identify monozygotic twins. BMC Oral Health, 20: 268.
66. Mou QN, Ji LL, Liu Y, Zhou PR, Han MQ, Zhao JM, Cui WT, Chen T, Du SY, Hou YX, Guo YC. (2021) Three-dimensional superimposition of digital models for individual identification. Forensic Sci Int, 318: 110597.
67. Thomas C, Kotze T, Nash J. (1986) The palatal ruga pattern in possible paternity determination. J Forensic Sci, 31: 288-292.
68. Revilla-Leon M, Frazier K, da Costa JB, Kumar P, Duong ML, Khajotia S, Urquhart O, Council on Scientific A. (2021) Intraoral scanners: An American Dental Association Clinical Evaluators Panel survey. J Am Dent Assoc, 152: 669-670 e662.
69. Taneva ED, Johnson A, Viana G, Evans CA. (2015) 3D evaluation of palatal rugae for human identification using digital study models. J Forensic Dent Sci, 7: 244-252.
70. Taneva E, Evans C, Viana G. (2017) 3D Evaluation of Palatal Rugae in Identical Twins. Case Rep Dent, 2017: 2648312.
71. Winkler J, Gkantidis N. (2021) Intraoral scanners for capturing the palate and its relation to the dentition. Sci Rep, 11: 15489.
72. Li J, Moon HS, Kim JH, Yoon HI, Oh KC. (2022) Accuracy of impression-making methods in edentulous arches: An in vitro study encompassing conventional and digital methods. J Prosthet Dent, 128: 479-486.
73. Gutmacher Z, Kelly A, Renne W, Hoover M, Mennito A, Teich S, Cayouette M, Ludlow M. (2021) Evaluation of the accuracy of multiple digital impression systems on a fully edentulous maxilla. Quintessence Int, 52: 488-495.
74. Giri J, Bockmann M, Brook A, Gurr A, Palmer L, Brook O'Donnell M, Hughes T. (2024) Relative contributions of genetic and environmental factors to palatal morphology: a longitudinal twin study. Eur J Orthod, 47.

75. Šidlauskienė M, Papievis V, Šidlauskas A, Šidlauskas M, Juzėnas S, Lopatienė K. (2024) Genetic and environmental impact on variation in the palatal dimensions in permanent dentition: a twin study. Sci Rep, 14: 19785.
76. Chiam TL, Perkins H, Hughes T, Palmer L, Higgins D. (2025) Palatal morphology: A systematic review of the association of palatal shape with genetic ancestry, sex and age. Arch Oral Biol, 175: 106275.
77. Azab SMS, Magdy R, Sharaf El Deen MA. (2016) Patterns of palatal rugae in the adult Egyptian population. Egypt J Forensic Sci, 6: 78-83.
78. Shetty SK, Kalia S, Patil K, Mahima VG. (2005) Palatal rugae pattern in Mysorean and Tibetan populations. Indian J Dent Res, 16: 51-55.
79. Borbola D, Berkei G, Simon B, Romanszky L, Sersli G, DeFee M, Renne W, Mangano F, Vag J. (2023) In vitro comparison of five desktop scanners and an industrial scanner in the evaluation of an intraoral scanner accuracy. J Dent, 129: 104391.
80. Vitai V, Nemeth A, Solyom E, Czumbel LM, Szabo B, Fazekas R, Gerber G, Hegyi P, Hermann P, Borbely J. (2023) Evaluation of the accuracy of intraoral scanners for complete-arch scanning: A systematic review and network meta-analysis. J Dent, 137: 104636.
81. Gibelli D, De Angelis D, Pucciarelli V, Riboli F, Ferrario VF, Dolci C, Sforza C, Cattaneo C. (2018) Application of 3D models of palatal rugae to personal identification: hints at identification from 3D-3D superimposition techniques. Int J Legal Med, 132: 1241-1245.
82. Zhao J, Du S, Liu Y, Saif BS, Hou Y, Guo YC. (2022) Evaluation of the stability of the palatal rugae using the three-dimensional superimposition technique following orthodontic treatment. J Dent, 119: 104055.
83. Eggmann F, Blatz MB. (2024) Recent Advances in Intraoral Scanners. J Dent Res, doi:10.1177/00220345241271937: 220345241271937.
84. Corte-Real A, Ribeiro R, Almiro PA, Nunes T. (2024) Digital Orofacial Identification Technologies in Real-World Scenarios. Applied Sciences-Basel, 14.

85. Corte-Real A, Ribeiro R, Machado R, Silva AM, Nunes T. (2024) Digital intraoral and radiologic records in forensic identification: Match with disruptive technology. Forensic Sci Int, 361: 112104.
86. Boedeker P, Kearns NT. (2019) Linear Discriminant Analysis for Prediction of Group Membership: A User-Friendly Primer. Adv. Methods Pract. Psychol. Sci., 2: 250-263.
87. Ramspek CL, Jager KJ, Dekker FW, Zoccali C, van Diepen M. (2021) External validation of prognostic models: what, why, how, when and where? Clin Kidney J, 14: 49-58.
88. Ho SY, Phua K, Wong L, Bin Goh WW. (2020) Extensions of the External Validation for Checking Learned Model Interpretability and Generalizability. Patterns (N Y), 1: 100129.
89. Abdellatif AM, Awad SM, Hammad SM. (2011) Comparative study of palatal rugae shape in two samples of Egyptian and Saudi children. Pediatr. Dent. J., 21: 123-128.
90. Santos C, Caldas IM. (2012) Palatal rugae pattern in a Portuguese population: a preliminary analysis. J Forensic Sci, 57: 786-788.
91. Byatnal A, Byatnal A, Kiran AR, Samata Y, Guruprasad Y, Telagi N. (2014) Palatoscopy: An adjunct to forensic odontology: A comparative study among five different populations of India. J Nat Sci Biol Med, 5: 52-55.
92. Kommalapati RK, Katuri D, Kattappagari KK, Kantheti LPC, Murakonda RB, Poosarla CS, Chitturi RT, Gontu SR, Baddam VRR. (2017) Systematic Analysis of Palatal Rugae Pattern for Use in Human Identification between Two Different Populations. Iran J Public Health, 46: 602-607.
93. Thomas C, Kotze T, Van der Merwe C. (1987) An improved statistical method for the racial classification of man by means of palatal rugae. Arch Oral Biol, 32: 315-317.
94. Burris B, Harris E. (1998) Identification of race and sex from palate dimensions. J Forensic Sci, 43: 959-963.
95. Lu C, Ahmed R, Lamri A, Anand SS. (2022) Use of race, ethnicity, and ancestry data in health research. PLOS Glob Public Health, 2: e0001060.

96. Ross PT, Hart-Johnson T, Santen SA, Zaidi NLB. (2020) Considerations for using race and ethnicity as quantitative variables in medical education research. Perspect Med Educ, 9: 318-323.
97. Information CIfH. (2020) Proposed Standards for Race-Based and Indigenous Identity Data Collection and Health Reporting in Canada https://lmaloles.vccdigitalmedia.ca/phpkit/wp-content/uploads/2024/11/CIHI-report-with-recommendations-in-ethnicity-and-Indigenous-status-data-collection.pdf date of access: 17.02.2026.
98. Bonham VL, Green ED, Pérez-Stable EJ. (2018) Examining How Race, Ethnicity, and Ancestry Data Are Used in Biomedical Research. JAMA, 320: 1533-1534.
99. Witzig R. (1996) The medicalization of race: scientific legitimization of a flawed social construct. Ann Intern Med, 125: 675-679.
100. Ousley S, Jantz R, Freid D. (2009) Understanding race and human variation: why forensic anthropologists are good at identifying race. Am J Phys Anthropol, 139: 68-76.
101. Nagare SP, Chaudhari RS, Birangane RS, Parkarwar PC. (2018) Sex determination in forensic identification, a review. J Forensic Dent Sci, 10: 61-66.
102. Santos F, Guyomarc'h P, Bruzek J. (2014) Statistical sex determination from craniometrics: Comparison of linear discriminant analysis, logistic regression, and support vector machines. Forensic Sci Int, 245: 204 e201-208.
103. Mikolicz Á, Simon B, Roudgari A, Shahbazi A, Vág J. (2024) Human identification via digital palatal scans: a machine learning validation pilot study. BMC Oral Health, 24: 1381.
104. Mikó S, Shahbazi A, Pellei D, Simon B, Vág J. (2025) Development of an experimental model for assessment of palatal tissue decomposition by intraoral scanner. Forensic Sci Int, 366: 112303.
105. Simon B, Mangano FG, Pal A, Simon I, Pellei D, Shahbazi A, Vag J. (2023) Palatal asymmetry assessed by intraoral scans: effects of sex, orthodontic treatment, and twinning. A retrospective cohort study. BMC Oral Health, 23: 305.
106. Saadeh M, Macari A, Haddad R, Ghafari J. (2017) Instability of palatal rugae following rapid maxillary expansion. Eur J Orthod, 39: 474-481.

107. Petju M, Suteerayongprasert A, Thongpud R, Hassiri K. (2007) Importance of dental records for victim identification following the Indian Ocean tsunami disaster in Thailand. Public Health, 121: 251-257.
108. Al-Hassiny A, Végh D, Bányai D, Végh Á, Géczi Z, Borbély J, Hermann P, Hegedüs T. (2023) User Experience of Intraoral Scanners in Dentistry: Transnational Questionnaire Study. Int Dent J, 73: 754-759.
109. Zarone F, Ruggiero G, Ferrari M, Mangano F, Joda T, Sorrentino R. (2020) Accuracy of a chairside intraoral scanner compared with a laboratory scanner for the completely edentulous maxilla: An in vitro 3-dimensional comparative analysis. J Prosthet Dent, 124: 761.e761-761.e767.
110. Vag J, Renne W, Revell G, Ludlow M, Mennito A, Teich ST, Gutmacher Z. (2021) The effect of software updates on the trueness and precision of intraoral scanners. Quintessence Int, 52: 636-644.
111. Weber-Lehmann J, Schilling E, Gradl G, Richter DC, Wiehler J, Rolf B. (2014) Finding the needle in the haystack: differentiating "identical" twins in paternity testing and forensics by ultra-deep next generation sequencing. Forensic Sci Int Genet, 9: 42-46.
112. Mennito AS, Evans ZP, Nash J, Bocklet C, Lauer Kelly A, Bacro T, Cayouette M, Ludlow M, Renne WG. (2019) Evaluation of the trueness and precision of complete arch digital impressions on a human maxilla using seven different intraoral digital impression systems and a laboratory scanner. J Esthet Restor Dent, 31: 369-377.
113. Vag J, Stevens CD, Badahman MH, Ludlow M, Sharp M, Brenes C, Mennito A, Renne W. (2023) Trueness and precision of complete arch dentate digital models produced by intraoral and desktop scanners: An ex-vivo study. J Dent, 139: 104764.
114. Roth I, Czigola A, Feher D, Vitai V, Joos-Kovacs GL, Hermann P, Borbely J, Vecsei B. (2022) Digital intraoral scanner devices: a validation study based on common evaluation criteria. BMC Oral Health, 22: 140.
115. Kanjanasavitree P, Thammajaruk P, Guazzato M. (2022) Comparison of different artificial landmarks and scanning patterns on the complete-arch implant intraoral digital scans. J Dent, 125: 104266.

116. Bing L, Kwon TG, Xiao W, Kyung HM, Yun KM, Wu XP. (2017) Model Analysis of Anatomical Morphology Changes of Palatal Rugae Before and After Orthodontic Treatment. Int. J. Morphol., 35: 1224-1229.
117. Xiu-Ping W, Jian-Ning H, Pan F, Yu-Jin W, Li B. (2017) Analysis of Palatal Rugae Morphology Before and After Orthodontic Treatment by a Digital Image Recognition System. Int. J. Morphol., 35: 420-424.
118. Saadeh M, Ghafari JG, Haddad RV, Ayoub F. (2017) Sex prediction from morphometric palatal rugae measures. J Forensic Odontostomatol, 35: 9-20.
119. Mankapure PK, Barpande SR, Bhavthankar JD. (2017) Evaluation of sexual dimorphism in arch depth and palatal depth in 500 young adults of Marathwada region, India. J Forensic Dent Sci, 9: 153-156.
120. Simon B, Farid AA, Freedman G, Vag J. (2023) Digital Palate Analysis to Verify the MirrorTwin Phenomenon. Oral Health Vol. July p. 34, Oral Health Group
121. Forrest A. (2019) Forensic odontology in DVI: current practice and recent advances. Forensic Sci Res, 4: 316-330.
122. Jayakrishnan JM, Reddy J, Vinod Kumar RB. (2021) Role of forensic odontology and anthropology in the identification of human remains. J Oral Maxillofac Pathol, 25: 543-547.
123. Sorrentino R, Ruggiero G, Leone R, Di Mauro MI, Cagidiaco EF, Joda T, Lo Russo L, Zarone F. (2024) Influence of different palatal morphologies on the accuracy of intraoral scanning of the edentulous maxilla: A three-dimensional analysis. J Prosthodont Res, 68: 634-642.
124. Xiong H, Li K, Tan K, Feng Y, Zhou JT, Hao J, Ying H, Wu J, Liu Z. (2023) TSegFormer: 3D Tooth Segmentation in Intraoral Scans with Geometry Guided Transformer. pp. 421-432, Springer Nature Switzerland, Cham
125. Zhang X, Luo Q, Shangguan H, Wu Y, Li B, Yang J. (2021) Three-dimensional palatal rugae recognition based on cyclic spectral analysis. Biomed Signal Process Control, 68: 102718.
126. Makrygiannakis MA, Vastardis H, Athanasiou AE, Halazonetis DJ. (2022) Novel method to delineate palatal rugae and assess their complexity using fractal analysis. Sci Rep, 12: 21749.

127. Bjelopavlovic M, Schmeisser F, Abou-Ayash S, Dengel A, Ahmed S, Erbe C, Petrowski K. (2026) Development and Validation of an Automated Algorithm for Palatal Rugae Matching in Forensic Identification. J Dent: 106311.
128. Adeniyi AO, Arowoogun JO, Okolo CA, Chidi R, Babawarun O. (2024) Ethical considerations in healthcare IT: A review of data privacy and patient consent issues. WJARR, 21: 1660-1668.
129. Dhirani LL, Mukhtiar N, Chowdhry BS, Newe T. (2023) Ethical dilemmas and privacy issues in emerging technologies: A review. Sensors, 23: 1151.

9 BIBLIOGRAPHY OF PUBLICATIONS

9.1 Publications related to the thesis:

Mikolicz A, Simon B, Gáspár O, Shahbazi A, Vag J. *Reproducibility of the digital palate in forensic investigations: a two-year retrospective cohort study on twins.* Journal of Dentistry. 2023 Aug;135:104562. doi: 10.1016/j.jdent.2023.104562. Epub 2023 May 24. PMID: 37230239.
Impact factor: 4.8 (ranking: D1)

Mikolicz Á, Simon B, Roudgari A, Shahbazi A, Vág J. *Human identification via digital palatal scans: a machine learning validation pilot study.* BMC Oral Health. 2024 Nov 14;24(1):1381. doi: 10.1186/s12903-024-05162-0. Erratum in: BMC Oral Health. 2024 Dec 23;24(1):1544. doi: 10.1186/s12903-024-05234-1. PMID: 39543590; PMCID: PMC11566520.
Impact factor: 3.1 (ranking: Q1)

Mikolicz Á, Simon B, Lőrincz G, Vág J. *Clinical precision of Aoralscan 3 and Emerald S on the palatal and dentition areas: Evaluation for forensic applications.* Journal of Dentistry. 2025 Feb;153:105455. doi: 10.1016/j.jdent.2024.105455. Epub 2024 Nov 8. PMID: 39522860.
Impact factor: 5.5 (ranking: D1)

Borbola D, Mikolicz A, Romanszky L, Sersli G, DeFee M, Renne W, Vag J. *Complete-arch accuracy of seven intraoral scanners measured by the virtual-fit method.* Journal of Dentistry. 2024 Oct;149:105281. doi: 10.1016/j.jdent.2024.105281. Epub 2024 Jul 31. PMID: 39094976.
Impact factor: 5.5 (ranking: D1)

Vág J, Nagy Z, Bocklet C, Kiss T, Nagy Á, Simon B, Mikolicz Á, Renne W. *Marginal and internal fit of full ceramic crowns milled using CADCAM systems on cadaver full*

arch scans. BMC Oral Health. 2020 Jul 6;20(1):189. doi: 10.1186/s12903-020-01181-9. PMID: 32631333; PMCID: PMC7339429.
Impact factor: 2.757 (ranking: Q1)

Vág J, Nagy Z, Simon B, Mikolicz Á, Kövér E, Mennito A, Evans Z, Renne W. *A novel method for complex three-dimensional evaluation of intraoral scanner accuracy.* Int J Comput Dent. 2019;22(3):239-249. PMID: 31463488.
Impact factor: 1.714 (ranking: Q2)

9.2 Publications not related to the thesis

Nagy Z, Mikolicz A, Vag J. *In-vitro accuracy of a novel jaw-tracking technology*. Journal of Dentistry. 2023 Nov;138:104730. doi: 10.1016/j.jdent.2023.104730. Epub 2023 Sep 28. PMID: 37777084.
Impact factor: 4.8 (co-first author) (ranking: D1)

Cumulative impact factor: 28,171

10 ACKNOWLEDGEMENTS

I would like to express my deepest gratitude to my supervisor, Professor János Vág, for his guidance and support, which were essential to completing this thesis. His incredible knowledge, scientific approach, and motivating attitude inspired me to pursue my Ph.D. His invaluable, insightful advice was essential in preparing and elevating the quality of this work.

I would also like to thank my former TDK student, Dr. Orsolya Gáspár, for her invaluable assistance during the research phase, which greatly facilitated the entire process. I also want to thank my other TDK student, Dr. Abdrabu Abdulrhman Ahmed, for his help with evaluating the results. Thanks also go to Dr. Petra Papp, Dr. Klaudia Lipták and Dr. Laura Lipták for their help with the examinations.

I would like to sincerely thank the twins and everyone involved in this research.

Many thanks to Dr Eszter Szalai and Dr Beáta Kerémi for their invaluable help and comments, which have greatly improved the quality of this thesis.

My gratitude also extends to the students, assistants and colleagues who were involved in this research, as well as to my parents and family for their persistent support.

Special thanks to the Science Management Workgroup of the Doctoral School at Semmelweis University for their invaluable guidelines and tips for writing my dissertation and improving its quality.